Aus dem Institut für Anatomie und Zellbiologie

Abteilung Medizinische Zellbiologie

Geschäftsführender Direktor: Prof. Dr. Ralf Kinscherf

des Fachbereichs Medizin der Philipps-Universität Marburg

Lack of influence of pituitary adenylate cyclase-activating peptide and PAC1 deficiency on astroglial signatures of apolipoprotein E-deficient mice under standard or high cholesterol diet

Inaugural-Dissertation

zur Erlangung des Doktorgrades der Zahnmedizin

dem Fachbereich Medizin der Philipps-Universität Marburg vorgelegt

von

Sophia Baki aus Bergisch Gladbach

Marburg, 2023

Angenommen vom Fachbereich Medizin der Philipps-Universität Marburg am:

27.02.2023

Gedruckt mit Genehmigung des Fachbereichs Medizin

Dekanin: Prof. Dr. Denise Hilfiker-Kleiner

Referent: Prof. Dr. Eberhard Weihe

Korreferent: Prof. Dr. Czubayko

Table of Contents

List of Tables

Table of Figures

List of Abbreviations

Abbreviation	Meaning
AB	Antibody
AD	Alzheimer's disease
aNSC	Adult neuronal stem cell
ApoE	Apolipoprotein E
AB	Antibody
cAMP	Cyclic adenosine monophosphate
CC	Corpus callosum
CNS	Central nervous system
DAB	3,3'-diaminobenzidine
DG	Dentate gyrus
GFAP	Glial fibrillary acidic protein
HCD	High cholesterol diet
HE	Hematoxylin eosin stain
(v)LDL	(very) Low density protein
MS	Multiple sclerosis
PA	Primary antibody
PACAP	Pituitary adenylate cyclase activating polypeptide
PAC1	PACAP type I receptor
PBS	Phosphate-buffered saline
PFA	Paraformaldehyde
SA	Secondary antibody
SD	Standard diet
SGZ	Subgranular zone

TBS	Tris-buffered saline
VC	Visual cortex
WT	Wildtype

1. Introduction

Because of its major contributions to largely untreatable, age-related conditions such as cardiovascular and neurodegenerative diseases, atherosclerosis is regarded as one of the leading causes of death worldwide (Chen et al., 2016; X. Li et al., 2011) and has often been associated with a typical western diet high in fat intake (Shoelson et al., 2007; Usui et al., 2012; Waqar et al., 2010). With our population rapidly aging and with obesity being a major health concern in the western world (Shoelson et al., 2007), the aforementioned illnesses are expected to increase in prevalence.

The pathogenesis of atherosclerosis is characterized by chronic sterile inflammation and microglial as well as astroglial activation (Cerami & Perani, 2015; Escartin et al., 2021; Groh et al., 2018). In atherosclerotic vascular disease and ischemic stroke, imaging of neuroinflammation suggests the activation of two different microglia subtypes which aid in disease progression (Cerami & Perani, 2015). Activation of microglia is regularly coupled to astroglial activation (Liu et al., 2020; Liu et al., 2011), which, in turn, is also related to obesity and can be seen in rodents fed with a diet high in fat (Buckman et al., 2013).

A major risk factor for atherosclerosis and neuroinflammatory diseases is the apolipoprotein E (ApoE) genotype (Davignon, 2005; Lahoz et al., 2001; Liu et al., 2013; Meir & Leitersdorf, 2004). ApoE protects the brain parenchyma from high cholesterol diet induced neurodegeneration by stabilizing the integrity of the blood-brain barrier (BBB; Meir & Leitersdorf, 2004; Mulder et al., 2001). ApoE-deficient mice show elevated plasma cholesterol levels and spontaneous atherosclerotic lesions (Li et al., 2016). The ApoE gene is known to have three different alleles – ε2, ε3 and ε4 – with different implications towards ApoE plasma levels and lipid metabolism (Rasmussen, 2016). In men, carriers of ApoE ε2 or ε4 have significantly higher risk of cardiovascular disease (Lahoz et al., 2001).

Recent evidence suggests a pituitary adenylate cyclase activating polypeptide-(PACAP)-deficiency dependent aggravation of peripheral atherosclerosis in ApoE-deficient mice (Rasbach et al., 2019). Profound influences were seen on the structural, cellular and cellular molecular signatures of the peripheral vascular wall under the development of atherosclerosis. PACAP is a neuroprotective,

immunoregulatory and vasoregulatory neuropeptide (Sherwood et al., 2000; Vaudry et al., 2009) exerting its influence by modulating the function of various cells, including the activity of microglia and astroglia (Waschek, 2013). PACAP performs pleiotropic actions in hypertension, Alzheimer´s disease (AD) and cerebral ischemia (Han et al., 2015).

Despite its high prevalence, the entailed suffering and a vast body of literature devoted to its understanding, the exact pathogenic mechanisms underlying atherosclerosis-induced alterations in the brain remain unclear (Li et al., 2011). Hence, the present study seeks to contribute to the research by investigating the influence of PACAP signaling on atherosclerosis-associated astroglial signatures in mice brains, which, to the best of our knowledge, has not been done before. The aim of the study was to test whether PACAP- and/or (its receptor) PAC1-deficiency in ApoE-knockout mice determine presumed astroglial response signatures under standard diet (SD) vs. under high cholesterol diet (HCD). The astroglial marker glial fibrillary acidic protein (GFAP) was therefore analyzed by qualitative and quantitative immunohistochemistry on deparaffinized brain sections of wildtype mice (WT), ApoE single-knockout mice ($PACAP^{+/+}/ApoE^{-/-}$ and $PAC1^{+/+}/ApoE^{-/-}$; henceforth referred to as $ApoE^{-/-}$), PACAP and ApoE double-knockout mice ($PACAP^{-/-}/ApoE^{-/-}$) as well as PAC1 and ApoE double-knockout mice ($PAC1^{-/-}/ApoE^{-/-}$). Both, the number of astrocytes and the proportional area of astrocytes were assessed in the corpus callosum (CC), the dentate gyrus (DG) and the visual cortex (VC). Prior to the study report, the theoretical background will be elucidated.

1.1. Atherosclerosis

Atherosclerosis is a chronic immunoinflammatory, multifocal, fibroproliferative disease of large and medium-sized arteries (Falk, 2006; Glass & Witztum, 2001). Atherosclerosis starts when the endothelium becomes damaged; cholesterol, macrophages and other blood substances are then able to build up in the artery wall forming artery-narrowing plaques (Veseli et al., 2017; *Figure 1*). This causes the disruption of blood flow throughout the body, resulting in possibly life-threatening conditions such as stroke and heart attack (Falk, 2006). While it is

known that atherosclerosis is responsible for most ischemic events in the brain (Napoli & Palinski, 2005), increasing evidence suggests that mechanisms causing atherosclerosis are also involved in the pathogenesis of neurodegenerative diseases such as Alzheimer's disease (Napoli & Palinski, 2005; Więckowska-Gacek et al., 2021). Age-related cerebrovascular atherosclerosis – and atherosclerosis in general – may even drive neurodegenerative diseases (Napoli & Palinski, 2005). Thus, insight into the factors determining susceptibility to atherosclerosis could also be of interest for the understanding of the progression of neurodegenerative diseases (Napoli & Palinski, 2005).

Various studies link atherosclerosis to hypercholesterolemia and inflammation (Joossens, 1988; e.g. Tedgui & Mallat, 2006). The expression of proinflammatory chemokines and cytokines characterize early atherosclerotic changes (Libby, 2012; Tedgui & Mallat, 2006; Tracy, 1997). As many scientific theories also point to the importance of neuroinflammation in the pathogenesis of neurodegenerative diseases (Griffin, 2006), this could be the common denominator. Further studies identifying pathways of atherosclerosis-associated inflammation and dysfunction in the central nervous system (CNS) are necessary, for example, as implemented in the present study, by targeting astrocytes.

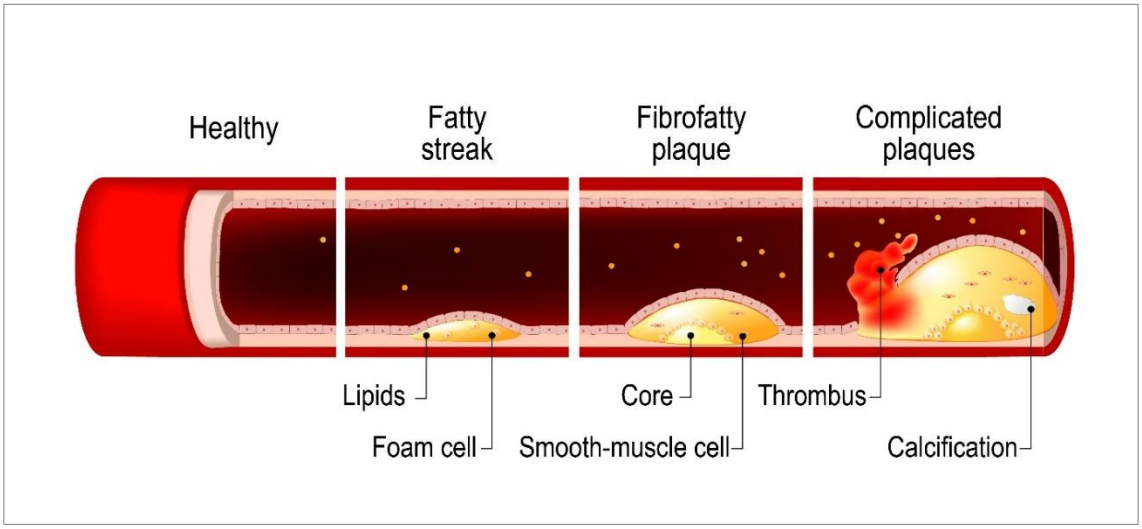

Figure 1. Stages of atherosclerosis. *First, lipids and foam cells form a fatty streak. As more cholesterol, macrophages and other blood substances start to build up, fibrofatty plaque is formed, eventually leading to complicated plaques including a thrombus and calcifications. Image adapted from Shutterstock downloaded (13.03.2022) with permissions.*

1.2. Astrocytes and neuroinflammation

Astrocytes, also known as astroglia, are specialized glial cells. They can be found throughout the entire CNS and outnumber neurons by a factor of five, functioning as their support (Sofroniew & Vinters, 2010). Astrocytes are decisively involved in many essential functions such as the formation of the BBB, the isolation of synapses, the exchange of molecules between neurons and the blood, ApoE production, the cholesterol supply of nervous cells and more (Jackson et al., 2021; Ringer et al., 2013; Sofroniew & Vinters, 2010).

Notably, astrocytes play a role in both neuroprotection and neurodegeneration (Sofroniew & Vinters, 2010). Besides their many functions in the healthy CNS, astrocytes respond to stress and damage in the nervous system with a process called astrogliosis (Sofroniew, 2015). Activated astroglia characteristically cumulate near damaged neurons and ß-amyloid plaques described by Alzheimer's disease (Griffin, 2006) and initiate an increase in the production of proinflammatory cytokines and chemokines (Li et al., 2011) (*Figure 2*). Generally, cell survival is reduced by proinflammatory cytokines which cause a shift from *neurogenesis* to *astrogliogenesis* (Kohman & Rhodes, 2013). In earlier research, it has not been determined whether increased astrocyte differentiation has a functional significance in stimulating the neuroinflammatory response, in the following recovery or both (Kohman & Rhodes, 2013). In recent studies, reactive astrocytes have been classified into A1 (the proinflammatory phenotype) and A2 (the anti-inflammatory phenotype) astrocytes (Fan & Huo, 2021). Therefore, these new classifications could possibly allow conclusions about neuroprotective or neurotoxic processes through the astrocyte signatures.

Neuroinflammation is associated with neurodegeneration, characterized by the slow and progressive dysfunction and loss of order and purpose in neuronal materials in the central nervous system (Chen et al., 2016) resulting in functional and mental impairments as observed in neurodegenerative disease such as Alzheimer's and Parkinson's (Amor et al., 2010; Griffin, 2006). The exact pathogenesis of most neurodegenerative diseases remains unknown, yet the importance of microglial and astroglial activation and their implications in

neuroinflammatory processes is emphasized by many scientists (Griffin, 2006; Li et al., 2011).

Another key player in the pathogenic mechanisms of atherosclerosis and neurodegenerative disease is thought to be ApoE (Huang & Mahley, 2014; Piedrahita et al., 1992), which is described in the following.

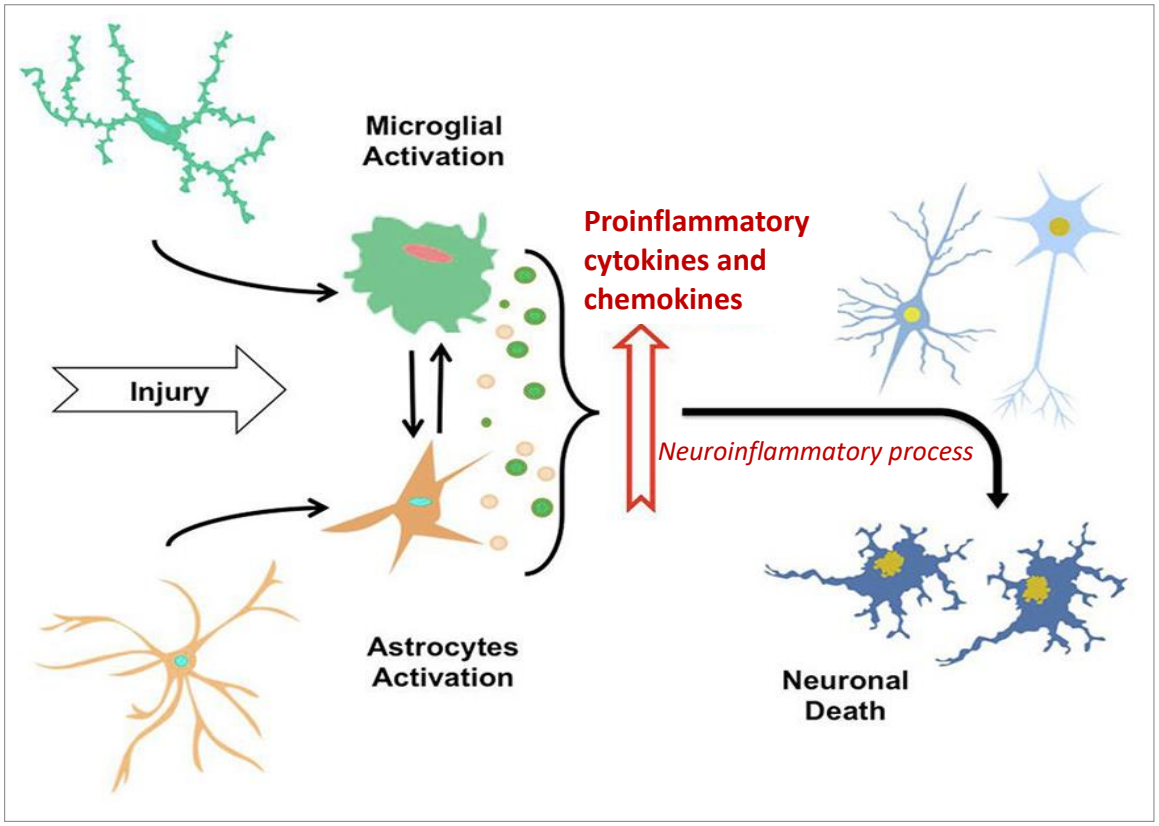

Figure 2. Astrocytes and microglia and the neuroinflammatory process. *In response to injury, both astrocytes and microglia become activated and initiate an increase in the production of proinflammatory cytokines and chemokines. Cell survival is reduced by proinflammatory cytokines, as the constant exposure to proinflammatory elements initiate a neuroinflammatory process eventually triggering neuronal death. Image adapted from Frontiers in Cellular Neuroscience, Morales et al. (2014).*

1.2.1. The link between ApoE-deficiency, a high cholesterol diet and atherosclerosis

ApoE is a glycoprotein playing an essential role in lipid metabolism (Huang & Mahley, 2014). It serves as a structural part of a very low-density lipoprotein (vLDL) and transports lipids between cells of different organs and tissues. Its main purpose is to mediate the binding of lipoproteins and lipid complexes (chylomicrons and vLDL) in the plasma or intestinal liquids to specific cell

receptors (LDL-receptors). In a study by Utermann et al. (1977) published in *Nature*, the role of a polymorphism in the ApoE gene in hyperlipoproteinaemia type III, a familial disorder associated with early-onset atherosclerosis, was demonstrated, henceforth rendering ApoE a key object of research in the investigation of hyperlipidemia. In a later study by Utermann and colleagues (1984), the authors were able to show a significantly higher frequency of ApoE alleles ε2 and ε4 in patients with hyperlipidemia, suggesting a higher susceptibility for hyperlipidemia in individuals carrying these alleles.

ApoE is primarily synthesized in the liver but also in macrophages, monocytes and astrocytes (Boyles et al., 1985; Huang & Mahley, 2014; Meir & Leitersdorf, 2004). In the brain specifically, most ApoE is synthesized by astrocytes (Boyles et al., 1985). ApoE-deficient mice ($ApoE^{-/-}$) show a fivefold increase in plasma cholesterol levels and spontaneous atherosclerotic lesions (Meir & Leitersdorf, 2004; Zhang et al., 1992). They develop lipid deposits in the proximal aorta from the third month on (Zhang et al., 1992). Xanthomatous lesions of the brain are first seen at the age of 17 months, consisting of crystalline cholesterol deposits, lipid globules and foam cells (Walker et al., 1997). ApoE-deficiency alone proves to be sufficient for atherosclerotic plaques to develop in mice (Greenow et al., 2005), however, diet might also play an important role (Nakashima et al., 1994). Nakashima et al. (1994), for instance, report an increased rate of atherogenesis in mice under HCD, which could be seen throughout the arterial tree, resulting in significant increases in plasma lipid levels, thereby highlighting the importance of hyperlipidemia in the development of atherosclerosis. ApoE-deficient mice fed with an HCD show atherosclerotic lesions (Li et al., 2016; Nakashima et al., 1994) and present the phenotype of an atherosclerotic mouse model (Li et al., 2016).

Besides its effect on lipid trafficking, ApoE may influence astroglial responses to damage in the CNS. For instance, significantly increased astrocyte and microglial activation in the hippocampus and cerebral cortex was found in mice under the influence of an HCD and in ApoE-knockout mice as compared to WT mice under SD (Crisby et al., 2004). HCD intake assumingly inhibits compensatory mechanisms of neuroinflammation and neurogenesis in the hippocampus (Janssen et al., 2016). Effects on lipid trafficking as well as effects on astrogliosis

may both account for a defective reinnervation often observed in ApoE$^{-/-}$ mice (Champagne et al., 2005).

As outlined above, animal models have provided great insight into underlying biological mechanisms of atherosclerosis (Li et al., 2011). Because of the tendency of the ApoE$^{-/-}$ mouse model towards spontaneous atherosclerotic lesions in mice under SD (Meir & Leitersdorf, 2004) and the comparability of these lesions to human lesions, the ApoE$^{-/-}$ mouse is a frequently used model not only in atherosclerosis but also in neurodegenerative diseases (Getz & Reardon, 2012; Rosenfeld et al., 2000; Yin & Wang, 2018). Therefore, ApoE-deficient mice were used as test animals in the present study as well.

1.3. Neuroprotective effects of PACAP

PACAP is part of the vasoactive intestinal peptide/glucagon/secretin superfamily and was originally isolated in the hypothalamus (Miyata et al., 1989). It is present throughout the entire central and peripheral nervous system as well as peripheral organs (Sherwood et al., 2000; Vaudry et al., 2009). PACAP is involved in brain development, the circadian rhythm, the respiratory and cardiovascular system, stress responses and inflammation (W. Liu et al., 2011; Vaudry et al., 2009; Waschek, 2013). It has been associated with physiological and pathophysiological processes related to neuroprotection (Rasbach et al., 2019) as well as various anti-inflammatory and cytoprotective properties (Miyata et al., 1989; Vaudry et al., 2009).

The neuroprotective effects of PACAP are primarily mediated through its specific receptor PAC1 (Harmar et al., 1998). The receptor is mainly expressed in the brain and in pancreatic β-cells (Jamen et al., 2000; Shen et al., 2013; Yamada et al., 2004), but has also been found in cardiac tissue and blood vessels (Gasz et al., 2006; Nandha et al., 1991). Its enormously good preservation throughout evolution emphasizes its crucial role in the regulation of essential biological functions (Sherwood et al., 2000).

Through its neuroprotective effects, PACAP can influence the course of neuronal injury, neurodegeneration and neuroinflammation (Dejda et al., 2005; Reglodi et

al., 2011). Protective effects of PACAP have been demonstrated in neurodegenerative diseases such as Alzheimer's disease (Rat et al., 2011), Parkinson's disease (Reglodi et al., 2004; Wang et al., 2008) and autoimmune encephalomyelitis (Tan et al., 2009). In models of brain injury, PACAP is upregulated in neurons and immune cells, promoting cell survival as well as regeneration and inhibiting apoptotic cell death (Dejda et al., 2005; Waschek, 2013). Studies investigating changes in PACAP and PAC1 receptor expression after CNS injury indicated an increase in PACAP in the pyramidal neurons of the cortex (Stumm et al., 2007) and in the ipsilateral dentate gyrus (Skoglösa et al., 1999). In addition, PACAP-deficient mice showed larger infarct size in cerebral ischemia (Seaborn et al., 2011).

PACAP exerts its neuroprotective actions either directly via activation of the cyclic adenosine monophosphate-(cAMP)-protein kinase A (PKA) pathway (Baxter et al., 2011) or indirectly by modulating glial cells to provide neuronal support with inflammatory responses (Masmoudi-Kouki et al., 2007). To protect neurons in ischemia, PACAP initiates astroglial cells, which have a lot of PACAP receptors, to release cytokines and chemokines (Dejda et al., 2005; Nakamachi et al., 2011).

Given the neuroprotective effects of PACAP and their involvement in neurodegeneration and neuroinflammation, it seems plausible to also assume PACAP to play a role in the process of atherosclerosis associated brain pathophysiology.

1.3.1. PACAP and atherosclerosis

There is numerous evidence linking atherosclerosis to diabetes (Chait & Bornfeldt, 2009) and the metabolic syndrome (Mathieu et al., 2006), with insulin resistance, glucose intolerance and other metabolic risk factors as their underlying cause (Grundy et al., 2004). PACAP stimulates insulin and glucagon secretion (Filipsson et al., 2015). It has been localized in pancreatic nerves and has been demonstrated to exert its actions directly in insulin-producing cells (Bertrand et al., 1996; De La Monte et al., 2009; Filipsson et al., 2015; Klinteberg et al., 1996). PACAP-deficient mice ($PACAP^{-/-}$) show reduced glucose-stimulated

insulin release and glucose tolerance after intravenous or gastric glucose injection (Sherwood et al., 2000). PAC1-deficient ($PAC1^{-/-}$) mice exhibit decreased PACAP-induced insulin secretion, indicating the receptor's influence on insulin secretion as well as glucose tolerance, and proving its importance in normal glucose homeostasis (Jamen et al., 2000). PACAP counteracts morphologic injury of endothelial and smooth muscle cells, inhibits the proliferation of smooth muscle cells and reduces lipid peroxides produced by endothelial cells and smooth muscle cells under hyperlipidemia (Chang, 1997). Moreover, it significantly increases the production of anti-atherosclerotic substances by endothelial cells, suggesting an anti-atherosclerotic potential (Chang, 1997). Additionally, recent studies on PACAP and PAC1 deficiency in ApoE-deficient mice ($PACAP^{-/-}$/$ApoE^{-/-}$ and $PAC1^{-/-}$/$ApoE^{-/-}$, double knockout mice) suggest PACAP as an endogenous atheroprotective neuropeptide (Rasbach et al., 2019) and PAC1 antagonists as anti-atherosclerotic drugs (Splitthoff et al., 2020). According to a recent study by Splitthoff et al, PAC1-deficiency in ApoE-deficient mice suppressed the accumulation and progression of atherosclerotic plaques after an HCD (Splitthoff et al., 2020). Further, Rasbach et. al, showed that a PACAP-deficiency in ApoE-deficient mice aggravated the formation and progression of atherosclerotic plaques (Rasbach et al., 2019).

1.4. The physiological and pathophysiological significance of brain regions selected for analysis in astrocyte responses

1.4.1. Corpus callosum

The corpus callosum (CC) (*Figure 3, Figure 4, Figure 5*) is the primary commissural region of the brain, consisting of white matter connecting the left and right cerebral hemispheres (Fitsiori et al., 2011; Goldstein et al., 2022). It consists of nearly 200 million strongly myelinated nerve fibers forming homotopical as well as heterotopical projections to contralateral neurons of the same anatomical regions (Goldstein et al., 2022). The main task of the CC is the integration and transfer of sensory, motor and cognitive information from both hemispheres (Goldstein et al., 2022).

In radiology, the CC serves as landmark for the differential diagnosis of neurological diseases since the location of lesions provides crucial information on the underlying pathology (Hattingen et al., 2010). As an example, in up to 93% of the cases, the CC is involved in multiple sclerosis (MS), an autoimmune, inflammatory demyelinating disorder (Hattingen et al., 2010). Even in earlier stages of MS, CC atrophy can be seen in magnetic resonance imaging (Pelletier et al., 2001). As the disease progresses, the CC undergoes further axonal degeneration and becomes more and more thinned out (Dietemann et al., 1988). The example of MS shows the vulnerability of the CC to inflammatory-driven diseases and thus justifies its inclusion in the present study: In MS lesions, lymphocytes, microglia and astroglia account for most of the cells in the inflammatory infiltrate (Buschmann et al., 2012). In response to oligodendrocyte stress as well as apoptosis, microglial activation and subsequent astrogliosis have been demonstrated to be increased in the CC compared to gray matter cortex regions (Buschmann et al., 2012).

Finally, infarcts of the CC are usually part of large vessel ischemia and mostly caused by cerebral embolisms, which makes studies like ours, investigating the effect of a high cholesterol diet and its implications in atherosclerosis, even more necessary (Chrysikopoulos et al., 1997).

1.4.2. Dentate gyrus

The dentate gyrus (DG) (*Figure 3, Figure 4, Figure 5)* is part of the hippocampus formation, a key structure of the limbic system playing an important role in pathological processes of neurodegenerative diseases such as AD (Bähr & Frotscher, 2003; Bandopadhyay et al., 2014). The DG consists of cerebral convolutions (gyri) and represents the entrance to the hippocampus (Amaral et al., 2007; Bähr & Frotscher, 2003). A remarkable feature of the DG (specifically, the subgranular zone, SGZ) is its ability for neurogenesis, existing lifelong in many vertebrates (Aimone et al., 2006; Gonzalez-Perez et al., 2010). New neurons are continuously added and appear to be associated with memory formation (Aimone et al., 2006). They are derived from adult neuronal stem cells (aNSC) with the ability to self-renew and differentiate into many kinds of cells

such as neurons, oligodendrocytes and astrocytes (Gonzalez-Perez et al., 2010). Studies have demonstrated an immunological control of aNSCs via cytokines and chemokines affecting proliferation, migration, differentiation, and cell survival, although signaling pathways are yet to be understood (Gonzalez-Perez et al., 2010). Interestingly, the primary progenitors giving rise to granular neurons in the SGZ are type-B cells, a subpopulation of astrocytes (Gonzalez-Perez et al., 2010). After kainate-induced seizures in mice dentate gyruses, the proliferation of these astrocytes is preferentially stimulated to increase neurogenesis (Hüttmann et al., 2003).

During inflammation of the hippocampus, complex modifications in the intercellular communication between neurons, microglia and astrocytes take place (Lana et al., 2017). In rats, lipopolysaccharide-induced inflammation in the SGZ leads to microglial and astroglial cooperation in the process of phagocytosis/phagoptosis of apoptotic granular neurons (Lana et al., 2017). Astrocytes develop longer branches, typical morphological features of reactive astrocytes (Lana et al., 2017). The differential activation of astrocytes as well as the alteration in their communication in the DG as compared to other hippocampal regions is assumed to be responsible for the specific susceptibility of the DG to neurodegeneration (Lana et al., 2017).

In entorhinal denervated rats, astroglial activation is characterized by proliferation, upregulation of GFAP and migration into the denervated zone of the DG (Rose et al., 1976). Increased expression of GFAP in astrocytes in the hippocampus is also found in rats fed with a hypercaloric diet (Bondan et al., 2019).

Besides immunological mediators, PACAP and ApoE have been implicated in neurogenesis in the hippocampus. In a study investigating adult mice hippocampal neurogenesis after stroke, PACAP promoted the proliferation of neuronal stem cells (Matsumoto et al., 2016). In young adult female mice with ApoE ε2 genotype, improved hippocampal progenitor cell proliferation has been found, whilst neurogenesis was reduced in ApoE ε4 carriers (Koutseff et al., 2014).

Taken together, the findings described above render the DG as an extraordinarily interesting region of interest, specifically with regard to astroglial responses in ApoE-, PACAP- and/or PAC1-knockout mice under HCD.

1.4.3. Visual cortex

The visual cortex (VC) (*Figure 3, Figure 4, Figure 5*) is located in the occipital lobe, the furthest dorsal part of the telencephalon (Huff et al., 2022). After passing through the thalamus and lateral geniculate nucleus, retinal information reaches the VC, where basal vision processes take place (Huff et al., 2022). The VC is one of the best-understood areas of the brain (Huff et al., 2022), which makes it an attractive region of interest.

Besides their neuromodulator-mediated global functions, astrocytes in the visual cortex show small but reliable responses to visual stimuli in awake mice with a five second delay compared to adjacent neurons, potentially pointing towards an intercellular communication (Sonoda et al., 2018). Furthermore, there is evidence implicating astrocytes in the modulation of visual cortex plasticity in response to vision loss (Hennes et al., 2020).

Compared to the CC and the DG, there is a much smaller body of research investigating inflammatory processes in the VC. Unsurprisingly, neuronal stress and neuronal loss in the visual cortex have been observed to be followed by an increase in (reactive) glia cells (Charleston et al., 1994; Devaney & Johnson, 1980). In late-stage AD, an upregulation of proinflammatory and proapoptotic gene expression can be found in the primary visual cortex (Cui et al., 2007). It is presumed that late-stage AD related visual disturbances like agnosia, visual hallucinations and face identification problems are a result of pro-inflammatory processes spreading along the pathway between the “entorhinal-primary visual cortex-thalamic-retinal axis” (Hill et al., 2014, p. 1).

While performing a thorough literature review neither studies investigating the effect of HCD on astroglial responses in the visual cortex, nor one investigating PACAP- or ApoE- deficiency, were present. Our study hence aims to expand the scientific knowledge in this area.

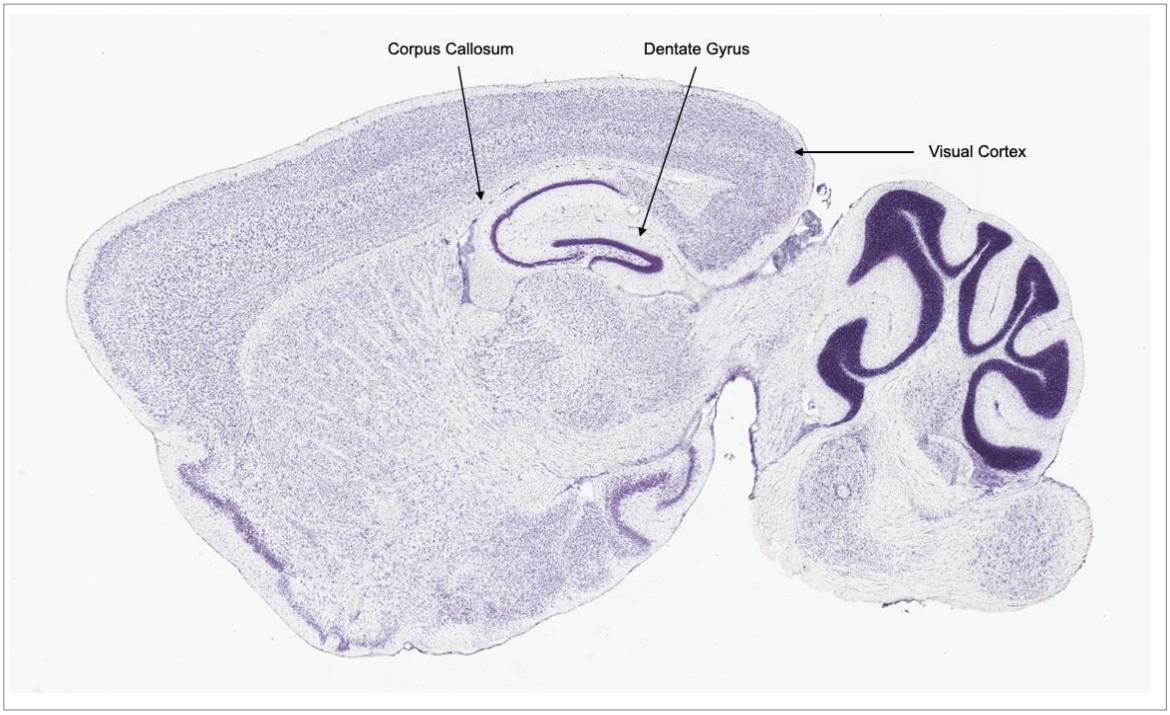

Figure 3. Mouse brain regions of interest. *Overview of the three mouse brain regions of interest, the corpus callosum, the dentate gyrus and the visual cortex. Sagittal cut; Nissl stain adapted from Allen Reference Atlas – Mouse Brain.*

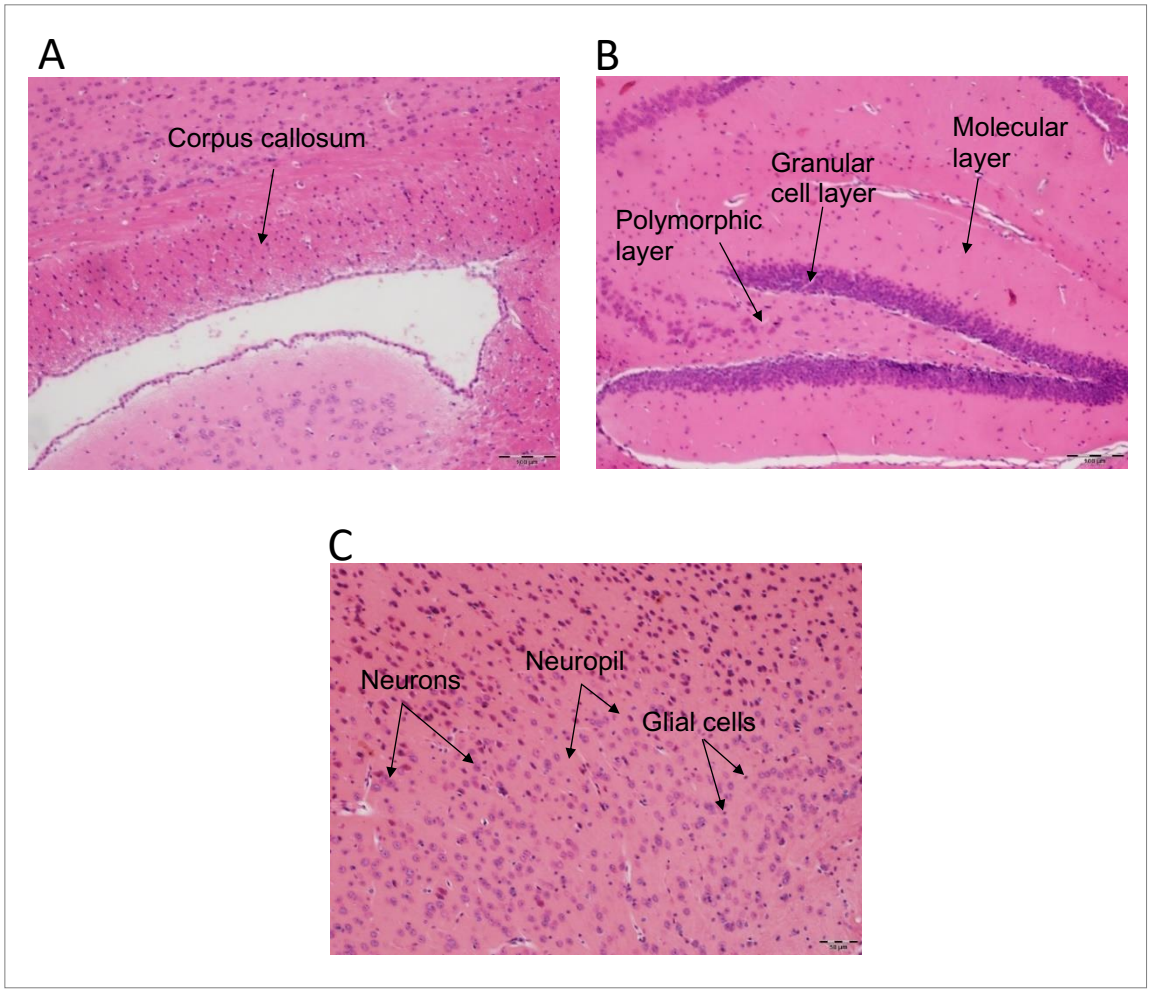

Figure 4. Giemsa stain of the brain regions investigated. *A: corpus callosum; B: dentate gyrus; the three layers of the DG, the polymorphic, the granular and the molecular cell layer C: visual cortex; for simplification purposes neurons, the neuropil and glial cells were just marked in the VC. Seen here: wildtype mice fed a high cholesterol diet in 100x enlargement (10x ocular and 10x lens).*

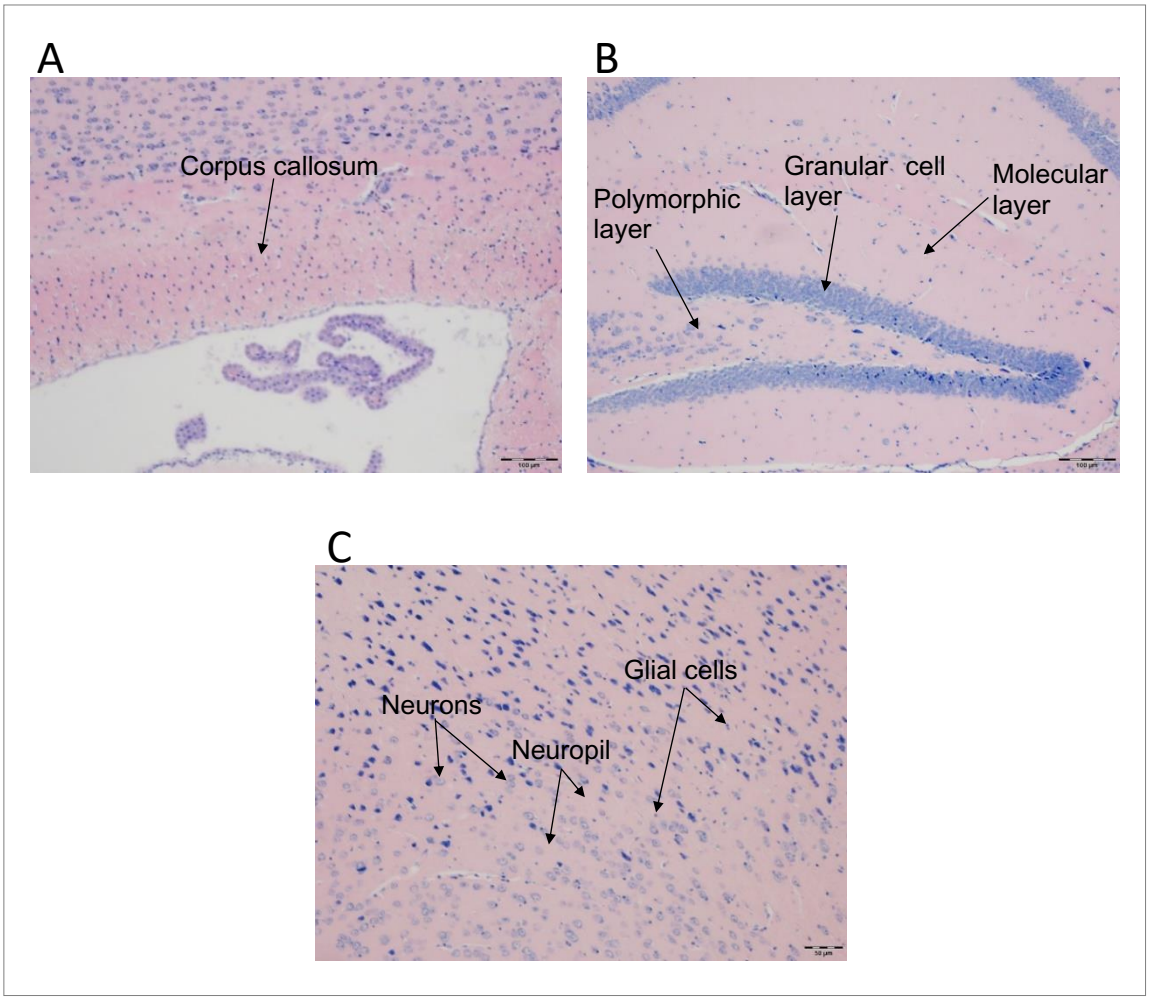

Figure 5. HE stain of the brain regions investigated. *A: corpus callosum; B: dentate gyrus; the three layers of the DG, the polymorphic, the granular and the molecular cell layer C: visual cortex; for simplification purposes neurons, the neuropil and glial cells were just marked in the VC. Seen here: wildtype mice fed a high cholesterol diet in 100x enlargement (10x ocular and 10x lens).*

2. Aims and hypotheses

In light of the previously mentioned involvement of PACAP and its specific PAC1 receptor in peripheral atherosclerosis in the ApoE model, it is the aim of the present study to test whether ApoE-, PACAP- and/or PAC1- deficiency in mice affects astroglial response signatures under SD (30 weeks SD) vs. HCD (10 weeks SD + 20 weeks HCD) in the CC, DG and VC. This research is essential given the recent evidence of a PACAP-dependent aggravation of atherosclerosis in ApoE-deficient mice (Rasbach et al., 2019) and PAC1 antagonists being suggested as anti-atherosclerotic drugs (Splitthoff et al., 2020). The study

hopefully contributes to the understanding of pathogenic mechanisms underlying atherosclerosis and the role of astrocytes within this framework. Moreover, the results might provide new insights as to whether PACAP receptor agonists and/or antagonists could offer new therapeutic options in the treatment of atherosclerosis-associated inflammation and dysfunction in the CNS, as PACAP has already been discussed as a therapeutic target in other inflammatory diseases (Abad et al., 2006) as well as in migraine (Zagami et al., 2014).

Given the preliminary findings, we hypothesize that ApoE-knockout mice show increased astrocyte numbers and proportional area of astrocytes as compared to WT mice. With regard to the study by Rasbach et al. (2019) and Splitthoff et al. (2020), PACAP$^{-/-}$/ApoE$^{-/-}$and PAC1$^{-/-}$/ApoE$^{-/-}$ double-knockout mice are expected to exhibit significantly stronger astroglial responses in comparison to ApoE single-knockout mice and WT mice.

HCD is generally expected to lead to an increase in astrocyte number and proportional area of astrocytes due to both, inflammatory processes (cf. Neustadt, 2006) and HCD-induced inhibition of compensatory mechanisms, specifically in the DG (Janssen et al., 2016). As previously shown by Crisby et al. (2004), ApoE-knockout mice under HCD are likely to show enhanced astroglial activation (hence, increased astrocyte number and proportional area of astrocytes) in comparison to WT mice under SD. The strongest astroglial response, however, is expected to be found in PACAP$^{-/-}$/ApoE$^{-/-}$and PAC1$^{-/-}$/ApoE$^{-/-}$ double-knockout mice under HCD.

With regard to the brain regions of interest, I assumed the largest astroglial response to be found in the DG versus the CC and VC. This assumption is based on the literature, where the DG has often been found to be particularly vulnerable (e.g. Lana et al., 2017).

3. Methods and materials

3.1. Experimental design

To investigate the influence of ApoE-, PACAP- and PAC1-deficiency on brain astroglia in the progression of atherosclerosis, brains from a total of *N* = 30 single- and double-gene deficient mice were analyzed. Gene-deficiency dependent atherosclerotic signatures at the peripheral vascular wall were determined in a separate study by Rasbach et al. (2019) and Splitthoff et al. (2020). Astrocyte count was assessed in homozygous wildtype (WT; serving as a control), ApoE-single-knockout (ApoE$^{-/-}$), PACAP and ApoE double-knockout (PACAP$^{-/-}$/ApoE$^{-/-}$) and PAC1 and ApoE double-knockout (PAC1$^{-/-}$/ApoE$^{-/-}$) mice. Astrocytes were counted in three different brain regions (CC, DG and VC) after labeling with glial fibrillary acidic protein (GFAP). The mice were either fed with an SD or an HCD. This resulted in eight subgroups of mice (*Table 1*).

Table 1. Subgroups of mice included in the study

	Standard diet	*N*		**High cholesterol diet**	*N*
Subgroup 1	WT mice	3	**Subgroup 2**	WT mice	4
Subgroup 3	ApoE$^{-/-}$ mice	3	**Subgroup 4**	ApoE$^{-/-}$ mice	4
Subgroup 5	PACAP$^{-/-}$/ApoE$^{-/-}$ mice	4	**Subgroup 6**	PACAP$^{-/-}$/ApoE$^{-/-}$ mice	4
Subgroup 7	PAC1$^{-/-}$/ApoE$^{-/-}$ mice	4	**Subgroup 8**	PAC1$^{-/-}$/ApoE$^{-/-}$ mice	4

3.2. Experimental animals

The rodents originated from the *Biomedical Research Centre* (Biomedizinisches Forschungszentrum, BMFZ; Hans-Meerwein-Straße 2, D-35043 Marburg; responsible: Guido Schemken) of the strain bred under barrier-maintained specific pathogen free husbandry. All ApoE$^{-/-}$ mice had a C57BL/6 background

(Bonaterra et al., 2012). Independent of their sex, homozygote *ApoE*^{tm1Unc} mice exhibit increased plasma cholesterol and triglyceride levels, however, without onerous effects on the animals. Lipid depositions in the proximal aorta develop from the third month of life. Accordingly, until the end of the period of observation (30 weeks) the phenotype stayed inconspicuous. Xanthomatous lesions appearing in the brains of mice consist of cholesterol deposits, lipid globules and foam cells and first progress at 17 months of age. In the present experiment, the mice did not reach the age of 17 months. Specific information on the different mice genotypes is presented in *Table 2* and can also be found in Rasbach et al. (2019) and Splitthoff et al. (2020).

Table 2. Specification of mice genotypes

	WT mice	**ApoE$^{-/-}$ mice**	**PACAP$^{-/-}$/ApoE$^{-/-}$ mice**	**PAC1$^{-/-}$/ApoE$^{-/-}$ mice**
Sex	Males	Males	Males	Males
Age	Ten weeks	Ten weeks	Ten weeks	Ten weeks
Breeding	C57BL/6 (*mus. Musculus L.*)	C57BL/6 *ApoE*^{tm1Unc} genetic background no strains (Bonaterra et al 2012)	Mice breed created by crossing ApoE$^{-/-}$ mice with PACAP$^{-/-}$ mice [PACAP$^{-/-}$ mice: C57BL/6 genetic background, no strains (Hamelink et al., 2002)] (breeding start: January 2013). No signs of strain determined through strain test by a group of Prof. Dr. Kinscherf.	Mice breed created by crossing ApoE$^{-/-}$ mice with PAC1$^{-/-}$ mice [PAC$^{-/-}$ mice: C57BL/6 genetic background, no strains (Hamelink et al., 2002)] (breeding start: March 2013). No signs of strain determined through strain test by a group of Prof. Dr. Kinscherf.

3.2.1. Ethical approval

By law, ethical approval was required for the present research project. In Germany, this is regulated by §40 (1) of the Medical Products Act (Arzneimittelgesetz; AMG), §20 (1) of the Medical Devices Act (Medizinproduktegesetz; MPG) and, specifically with regard to the protection of animals, by §15 (1) of the Animal Protection Act (Tierschutzgesetz; TierSchG). The regional authority in Giessen approved the application (V54-19 c 2015 h 01 MR 20/26 Nr.21/2014; for more information please visit: https://www.uni-giessen.de/fbz/fb11/dekanat/ethikkommission). Animals were treated with respect in terms of their status and needs as living beings and were sensitively looked after.

3.2.2. Diet

For the first ten weeks, all mice received the same standard diet with a fat content of 4.3% (SD; LASQCdiet® Rod16 Rad; LASvendi, Soest, Germany). During the following twenty weeks, each superordinate genotype group was divided into two feeding groups (*Table 1*). One group continued to be fed with an SD, while the other half was fed an HCD ("western-type diet") with a fat content of 21% and added cholesterol [HCD; (21 % fat, 0.15 % cholesterol and 19.5 % casein), Altromin GmbH, Lage, Germany].

3.3. Materials

For consumable supplies, equipment, chemicals and solutions as well as the software used in the study, please refer to *Table 3*-*Table 7* below.

Table 3. Consumable supplies

Name	Manufacturer
Cover slips	Carl Roth GmbH, Karlsruhe, Germany

DePeX mounting medium	SERVA Electrophoresis GmbH, Heidelberg, Germany
EDTA monovettes	Sarstedt AG & Co, Nümbrecht, Germany
Eppendorf tubes	Eppendorf AG, Hamburg, Germany
Microscope slides	Carl Roth GmbH, Karlsruhe, Germany
Reaction tubes	Sarstedt AG & Co, Nümbrecht, Germany
PAP Pen	Immunotech, Beckman Coulter Company, Marseilles, France
Pipette tips without filter	Sarstedt AG & Co, Nümbrecht, Germany

Table 4. Equipment

Name	**Manufacturer**
Autoclave	Fedegari Group, Albuzzano, Italien
Magnetic stirrer *MR Hei-Mix S MR 3001*	Thermo Fisher Scientific, Massachusetts, USA
Heating plate	MEDAX GmbH & Co.KG, Kiel, Germany
Induction cooker	Alaska e.K., Viernheim, Germany
Incubators	Heraeus Group, Hanau, Germany; BINDER GmbH, Tuttlingen, Germany
Cuvette holder	Eppendorf AG, Hamburg, Germany
Microscope *AX70*	Olympus, Tokyo, Japan
Microscope *BX40*	Olympus, Tokyo, Japan
Pipettes	Gilson, Middleton, USA; Eppendorf AG, Hamburg, Germany
Buffer chamber	INTEGRA Biosciences, Zizers, Switzerland
Rotation microtome *HM 325*	Leica Microsystems, Wetzlar, Germany
Stirrer *Heidolph MR 3001*	Sigma-Aldrich, Missouri, USA
Stopwatch	Carl Roth GmbH, Karlsruhe, Germany
SPOT camera	Diagnostics Instruments Inc., Seoul, South Korea
Vortex	IKA, Staufen im Breisgau, Germany

Scale *KERN 440-47N*	Kern & Sohn GmbH, Balingen, Germany
Centrifuge Biofuge pico	Thermo Fisher Scientific, Massachusetts, USA
Centrifuge Universal Multifuge 3L-R	Heraeus Group, Hanau, Germany
Centrifuge Perfect Spin P	PEQLAB Biotechnologie GmbH, Erlangen, Germany

Table 5. Chemicals

Name	**Description/manufacturer**
Aceton	Carl Roth GmbH, Karlsruhe Germany
Avidin, Biotin	Biozol, München, Germany
Aqua dist.	demineralized water cleaned by a TKA Ultrapure Water System (Niederelbert, Germany) on a cartridge
Azure eosin methylene blue (Giemsa's stain solution)	Merck, Darmstadt; Germany
Ultrapure water/analysis water	purified by a TKA Ultrapure Water System (Niederelbert, Germany)
Ultrapure water (B. Braun H_20)	B. Braun SE, Melsungen, Germany
Bovine serum albumin (BSA)	Serve, Heidelberg, Germany
Citric acid monohydrate	cat. no. 244; Merck KGaA, Darmstadt, Germany
DAB(3,3'-diaminobenzidine)	Sigma, Deisenhofen
Ethanol	Roth, Karlsruhe, Germany
Hematoxylin eosin stain (HE)	Merck, Darmstadt, Germany
Hydrogen peroxide (H_2O_2, 30%)	Carl Roth, Karlsruhe, Germany
Isopropanol	Merck, Darmstadt, Germany
Methanol	Merck, Darmstadt, Germany
Sodiumcitrate-dihydrate	cat. no. 6448; Merck KGaA, Darmstadt, Germany
Sodium chloride	Merck, Darmstadt, Gemany

Sodium dihydrogen phosphate	Merck, Darmstadt, Germany
Sodium phosphate	Merck, Darmstadt, Germany
Tris-sodium citrate	Merck, Darmstadt, Germany
TESAP (3-triethoxysilylpropylamine)	Merck, Darmstadt, Germany
Xylol	Merck, Darmstadt, Germany
Formaldehyde	Roth, Karlsruhe, Germany

Table 6. Solutions

Name	**Description/ composition**
Tris-buffered saline (TBS, 10x, rinsing buffer)	53g NaCl, 12g Tris, 1,000ml aqua dist., diluted 1:10, pH 7.4
Trisodiumcitrate dihydrate (10mM)	2.9410g/l, pH 6.0 (through HCl)
Paraformaldehyde (PFA) solution	4% (w/v) formaldehyde solution in phosphate-buffered saline; pH 7.2-7.4
Phosphate buffered saline solution (PBS)	6,55g NaH_2PO_4, 45g NaCL, 36,05g Na_2HPO_4 in 4,5l Aqua bidist.;with 1 M NaOH balance to pH 7,4, fill rest with Aqua bidist. to 5l
Peroxidase block	3ml H_2O_2 (30%) in 600ml methanol

Table 7. Software

Name	**Manufacturer**
SPSS Statistics, version 24	IBM Corp., New York, USA
SPOT Elite	Diagnostic Instruments Inc., Michigan, USA
ImageJ	Wayne Rasband, National Institute of Health, Maryland, USA
Word, Excel, PowerPoint (2008)	Microsoft Corp., Washington, USA

3.4. Procedure

3.4.1. Extraction of the tissues

After the mice were fed for a period of thirty weeks, they were anesthetized (Forene Abbott, Switzerland) and strongly narcotized through intraperitoneal application of a ketamine-xylazine-mixture (150mg/kg bodyweight ketamine + 20mg/kg bodyweight xylazine; Ketanest®/Rompun®). Hereafter, the thorax was opened and the left ventricle cannulated. Blood samples from the right atrium were taken and heparinized (0.25IU/ml). Blood plasma was extracted by centrifugation (10min, 650g) and stored at -80°C. The animals were perfused with PBS/heparin (0.01%) followed by exsanguination. Depending on the specific scientific question and the ongoing processing in the laboratory, there were different methods used for the fixation of the tissues and organs. The kidney and other organs were extracted from the opened abdomen and snap-frozen in liquid nitrogen-cooled isopentane and stored at -80°C until further use (data was analyzed and reported elsewhere). In the case of the present study, mice brains were fixated in paraformaldehyde and postfixed in bouin's solution (*Table 6*).

3.4.2. Silanization of the microscope slides

To ensure adherence of the tissue sections to the microscope slides, they were first washed and coated with TESAP. The slides were sorted into appropriate slide boxes and filled with 1.7l of hot water with a dash of rinsing agent. The boxes were then shaken on a plate shaker for an hour. In order to remove the rinsing agent sufficiently, they were washed three times with hot water, then washed once with demineralized water and finally washed with ultrapure water. The microscope slides were then cleaned for 45 minutes with 70% ethanol in ultrapure water and afterwards placed in the drying cabinet at 60°C to dry overnight. The next day, the slides were cleaned and ready to be coated. This was done by

immersion of the slides for 30 seconds first in TESAP and acetone, then twice in acetone, once in demineralized water and finally in double demineralized water. To dry, the silanizated slides were placed in a 42°C oven and then stored in dust-free boxes until further usage.

3.4.3. Cutting of the tissue sections

First, aqua bidist. was degassed for 30 minutes, filled into the two basins of the microtome and heated to 42°C for better stretching of the tissue sections. Each brain section was cut into ten to 15 7nm slices by means of the microtome and then drawn onto the silan-coated slides. Afterwards they were placed vertically on kitchen paper for excess water to drain off. To ensure complete drying and stretching of the tissue sections, they were dried for one hour on a 42°C heating plate and then dried overnight in a 60°C oven. The sections were stored at room temperature in appropriate slide boxes until further usage.

3.4.4. Immunohistochemistry

For the detection of astrocytes, the primary antibody (PA) GFAP (Progen Biotechnic GmbH, Heidelberg, Germany; dilution 1:3000; donor species: guinea pig) was used. By using a biotinylated secondary antibody (SA) (Dianova, Hamburg, Germany; dilution 1:200; donor species: donkey), the PA bound to the tissue was colored with the help of streptavidin-coupled avidin biotin peroxidases and DAB (brown precipitate, peroxidase substrate) and addition of nickel (blue-black precipitation, complexing agent).

Washing steps

Before staining in an aqueous solution the paraffin was removed (dewaxing) from the microscope slides using xylol, allowing the tissue to be stained. For this purpose, they were washed various times in xylol (three times) for ten minutes, then for 10 minutes in absolute isopropanol and subsequently in a peroxidase block (3ml H_2O_2 30% in 600ml methanol) for 30 minutes. The slides were then

stored in the fridge (6C°). Afterwards, they were placed in absolute isopropanol for ten minutes and then in descending concentrations of 96%, 80%, and 70% isopropanol, five minutes at a time. After two H_2O washings, each five minutes long, for antigen retrieval the slides were placed in a citrate buffer at 92-95°C for ten minutes, followed by one more washing step in H_2O.

Primary antibody

The procedure involved drying the microscope slides using a vacuum and circumscribing each histological section with a PAP-PEN, to create a hydrophobic barrier. Subsequently, the sections were individually dripped with 5% BSA-PBS for 30 minutes, then with 1% BSA-PBS for five minutes, followed with 30% avidin for 20 minutes. At this point, the endogenous biotin binding sites were neutralized. The histological preparations were then briefly dripped with 1% BSA-PBS, then covered with 30% biotin for the next 20 minutes and again dripped with 1% BSA-PBS for five minutes. This step neutralized the remaining avidin-binding sites. Between each of the steps, starting at the application of the PAP-PEN, the microscope slides were washed with H_2O and thereby cleaned before applying the next solution. Lastly, the primary antibody for visualization of GFAP (donor species: guinea pig; Progen Biotechnic GmbH, Heidelberg, Germany) in the dilution 1:3000 was applicated and left in an incubator at 16°C overnight.

Secondary antibody and AB-complex

On day two, the microscope slides were transferred from 16°C to 37°C for two hours, followed by washing steps to clean the remains of the PA (H_2O, three times aqua bidist. for five minutes, PBS-ICC for ten minutes). Then the histological sections were placed in 0.5%-BSA-PBS, dried with a vacuum and dampened with the biotinylated SA (donor species: donkey, Dianova, Hamburg, Germany) in the dilution 1:200. After incubation at 37°C for 45 minutes, the same washing steps as before were conducted. After washing in 0.5% BSA-PBS, the AB-complex was applicated (20µl solution A and 20µl solution B in 1ml 1% BSA-PBS pre-incubated for 30 minutes at room temperature) for 30 minutes at 37°C, followed by the same

washing steps as before. Meanwhile, DAB-aliquot (100mg) and Nickel-aliquot (600mg) were solved and filtrated in 800ml BPS-ICC. The slides were preincubated for five minutes before adding 112µl of H_2O_2 and leaving them in the solution for exactly eight minutes. After washing in aqua bidist. three times for five minutes and dehydration in ascending alcohol series of xylol three times, each for ten minutes, the slides were covered using DePeX.

Giemsa stain

For better oversight and distinct orientation throughout the histological preparations every tenth slide was colored in regular intervals, using the Giemsa staining method *(Figure 4)*. To accomplish this, in each case, after dewaxing as described above, hydration steps were performed in descending alcohol series (2x 100%, 1x 96%, 1x 90%, 1x 80%, 1x 70% alcohol), followed by aqua bidist. to rehydrate. Thereafter, they were immersed in a freshly made Giemsa solution for one hour. Through this, the intensity of the coloration was determined. The red tones were developed using four drops of CH_3COOH in 200ml aqua bidist. The same procedure was repeated to differentiate the blue tones with 96% alcohol. Finally, they were washed three times in absolute alcohol and xylene, each for five minutes, and covered using DePeX. Cell nuclei were plot in red, the cytoplasm in blue and the erythrocytes in orange.

Hematoxylin-eosin stain

The second coloring technique used was the hematoxylin-eosin (HE) stain (*Figure 5*). Through this technique, the cell nuclei were marked in blue, the cytoplasm in red and the erythrocytes orange. First, the slides went through similar steps as with the Giemsa staining method (dewaxing and hydration). Afterwards, they were placed in distilled water for five minutes and in hematoxylin for five to ten minutes. Under running water, the slides were blue annealed (increase in pH-value) and placed briefly in aqua bidist. For the red pigmentation, the preparations were placed in eosin for one minute. Then, again, they were washed in aqua dist. and for roughly 20 seconds in ascending alcohol series (1x

70%, 1x 80%, 1x 96% alcohol). Finally, for dehydration of the tissue sections, they were placed in absolute alcohol and xylene three times for five minutes and covered using DePeX.

Microscopy

The visualization of immunohistochemically stained tissue sections was carried out under the brightfield microscope (100x enlargement; 10x objective and 10x ocular). The images were captured with a digital camera and recorded with the image processing software SPOT Elite. A scale was inserted at the bottom right edge of each histological picture. For details on equipment and software please refer to *Table 4* and *Table 7.* After visual inspection, the most suitable slide of the CC, DG and VC was chosen for each mouse.

3.4.5. Image preprocessing and measurement of astrocyte signatures

Up to date, there are no efficient image analysis tools available to quantify astrocytes from large datasets (Suleymanova et al., 2018). As astrocytes are star-shaped with versatile branching structures, automated counting is rather difficult. Therefore, in the present study, astrocytes were counted twice using two different methods, subsequently calculating means. Counting was done using *ImageJ*, an open-source image processing software designed for scientific multidimensional images (see https://imagej.nih.gov/ij/, see also *Table 7*). The program allowed standardized counting, which was crucial in view of the number of cells and images to process.

Preprocessing was same for all images (*Figure 6*): After converting the image type to 8-bit, the threshold adjustment feature *triangle* was applied, thereby suppressing lower intensity pixels that do not represent cells. A binary image was obtained, with only two-pixel intensities. To be able to count the astrocytes while ignoring circular substructures within cells and any clusters identified as too small to be a cell, it was important to put in place a lower limit. Scaling was manually adjusted (ImageJ feature *known distance*) based on the 100µm marking on the right lower edge of each image, and the desired area was manually selected

according to the shape of the respective brain region (ImageJ feature *freehand selection*).

After preprocessing, the number of astrocytes and the proportional area of astrocytes was analyzed separately for each image:

Number of astrocytes: At this point, two different counting techniques were subsequently used in order to ensure data quality: For the first technique, the number of astrocytes in each image was analyzed individually, depending on the individual image composition (ImageJ feature *analyze particles*; setting: *[default]*[1]*-infinity*). Although, this procedure can be seen as subjective, it does take the individuality of every picture into consideration. For the second technique, astrocytes were counted in batch processing (ImageJ feature *analyze particles*; setting: *50-infinity*). The Pearson correlation between the two techniques was excellent (r = .94), therefore, mean values were calculated and used in the following analyses.

Proportional area of astrocytes: ImageJ was also used to measure the proportional area of astrocytes. The images were preprocessed as described above. The black pixels were then counted using the ImageJ feature *area fraction*. The results are presented in percentage per area.

[1] *[default]* = The setting was adjusted according to whether the cell bodies and its respective dendrites were identified as one cell by the software.

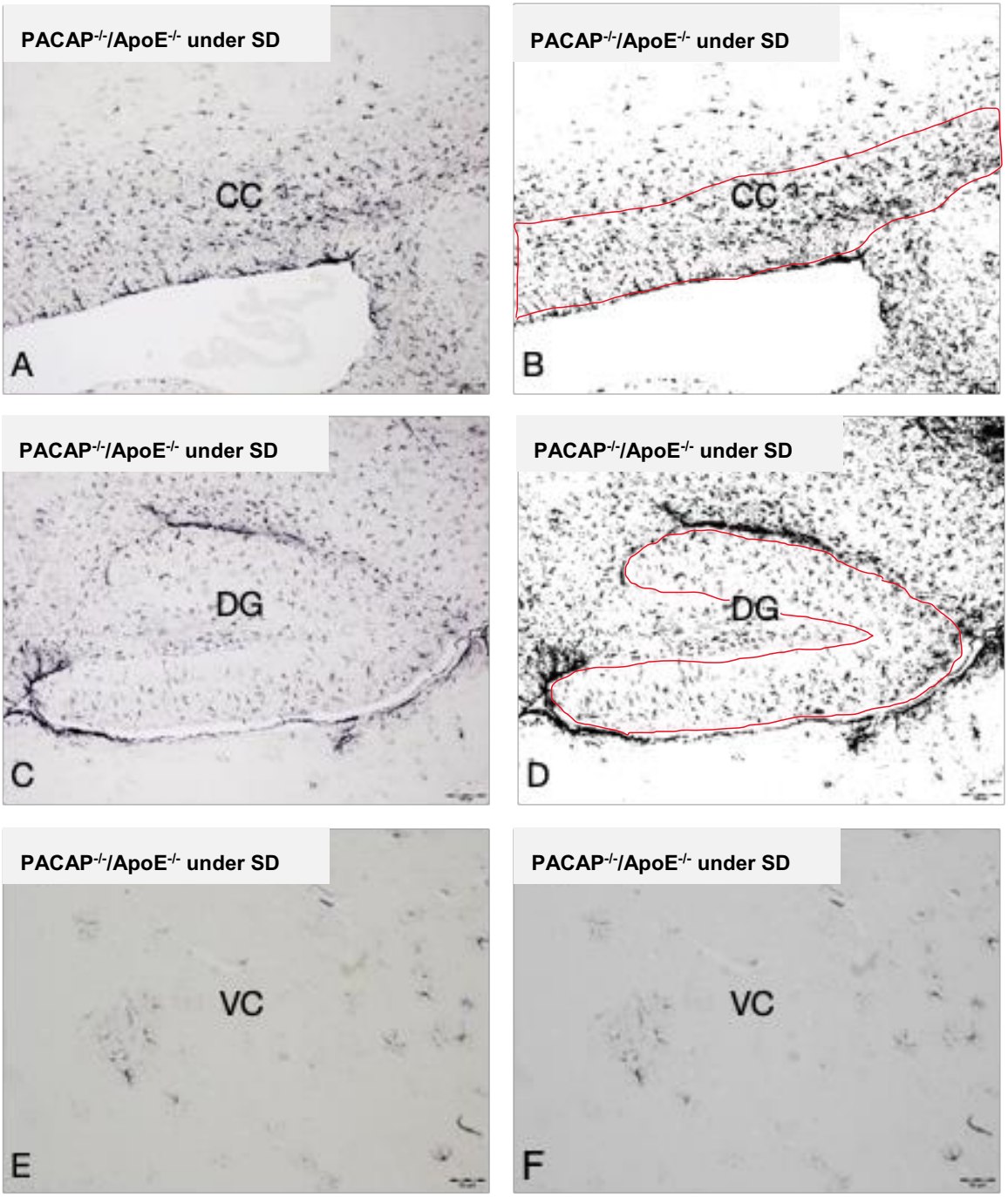

Figure 6. Stages of image preprocessing. *Shown here: PACAP$^{-/-}$/ApoE$^{-/-}$ mice under standard diet (SD). A, C, E: Before image preprocessing. B, D, F: After converting images to 8-bit, applying threshold, scaling, and marking the desired area of analysis. A and B: Corpus callosum (CC), C and D: Dentate gyrus (DG), E and F Visual cortex (VC)*

3.5. Statistical analysis

The statistical analysis was conducted using SPSS Statistics (*Table 7*). Descriptive statistics (mean, standard deviation) were calculated. After testing for

normality and variance homogeneity, multifactorial Kruskal-Wallis tests were performed to assess the statistical significance of group differences in astrocyte count and astrocyte percentage. Mann-Whitney U tests were used for post-hoc analysis. Alpha-error probability was set to $p < 0.05$. Multiple testing was controlled by Bonferroni correction. The analysis was separated into the three main factors (genotype, diet and brain region).

4. Results

4.1. Regional differences in astrocyte signatures in wildtype, ApoE$^{-/-}$-, PACAP$^{-/-}$/ApoE$^{-/-}$- and PAC1$^{-/-}$/ApoE$^{-/-}$ mice under standard and high cholesterol diet

In most of the genotypes regional differences in astrocyte signatures (number of astrocytes and proportional area of astrocytes) between the corpus callosum, the dentate gyrus and the visual cortex were observed. Results are described for mice fed an SD (30 weeks) and an HCD (10 weeks SD followed by 20 weeks HCD) individually and are presented for each genotype separately.

4.1.1. Wildtype mice

In wildtype mice fed with an SD significantly higher numbers of astrocytes in the DG compared to the VC were observed. No significant differences were seen when comparing the number of astrocytes of the CC and the DG as well as the CC and the VC. The proportional area of GFAP-stained astrocyte profiles in wildtype mice did not significantly differ between the three brain regions (*Figure 7*).

Under HCD, there was not only a significant difference in the number of astrocytes between the CC and the VC, but also between the DG and the VC. No significant difference was found when comparing the CC and the DG. Again the proportional area of astrocytes in wildtype mice did not significantly differ between the three brain regions (*Figure 7)*.

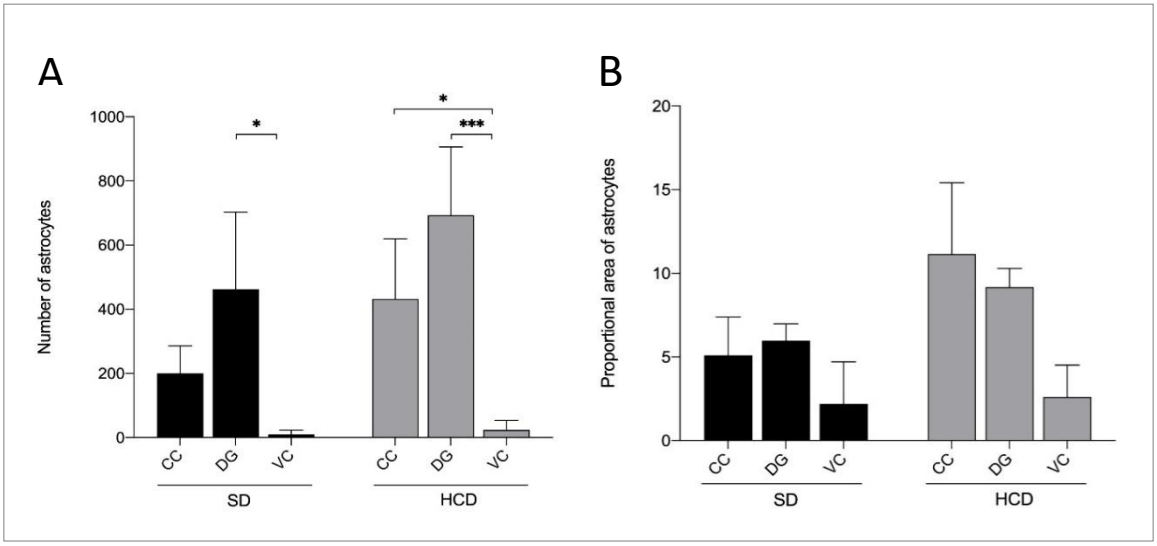

Figure 7. Regional differences in the number of astrocytes (A) and the proportional area of astrocytes (B) in wildtype mice under SD and HCD. *A. Left: Significantly larger number of astrocytes in the DG compared to the VC (Mann-Whitney-U test; $p < .05$) in WT mice under SD (N = 9); Right: Significantly larger number of astrocytes in the CC compared to the VC (Mann-Whitney-U test; $p < .05$) and in the DG compared to the VC (Mann-Whitney-U test; $p < .001$) in WT mice under HCD (N = 12). B. Left: No significant regional differences in WT mice under SD (N = 9). Right: No significant regional differences in WT mice under HCD (N = 12). Abbreviations: standard diet (SD), high cholesterol diet (HCD), corpus callosum (CC), dentate gyrus (DG), visual cortex (VC).*

4.1.2. ApoE$^{-/-}$ mice

Under SD there was a significantly higher number of astrocytes and a higher proportional area of astrocytes in the CC compared to the VC of ApoE$^{-/-}$ mice. The same was found when comparing the DG to the VC. There was no statistically significant difference in the number of astrocytes or the proportional area of astrocytes between the CC as compared to the DG (*Figure 8*).

In ApoE$^{-/-}$ mice under HCD there was a significantly higher number of astrocytes and a higher proportional area of astrocytes in the CC as well as the DG compared to the VC. There was no statistically significant difference in the number of astrocytes or the proportional area of astrocytes when comparing the CC to the DG (*Figure 8*).

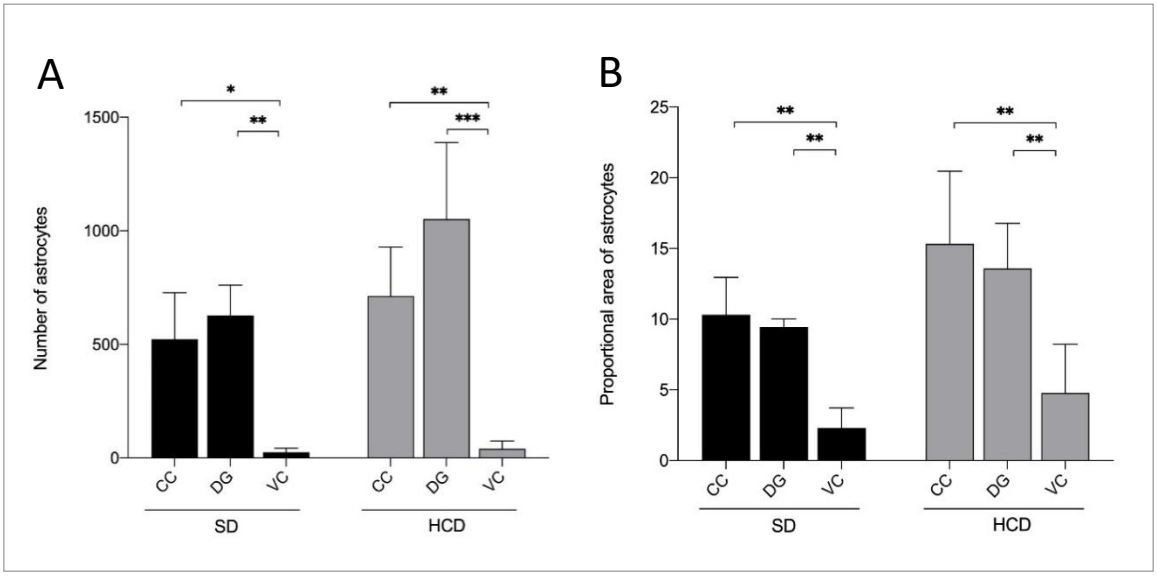

Figure 8. Regional differences in the number of astrocytes (A) and the proportional area of astrocytes (B) in ApoE$^{-/-}$ mice under SD and HCD. *A. Left: Significantly larger number of astrocytes in the CC compared to the VC (Mann-Whitney-U test; p < .05) and in the DG compared to the VC (Mann-Whitney-U test; p < .01) in ApoE$^{-/-}$ mice under SD (N = 9). Right: Significantly larger number of astrocytes in the CC compared to the VC (Mann-Whitney-U test; p < .01) and in the DG compared to the VC (Mann-Whitney-U test; p < .001) in ApoE$^{-/-}$ mice under HCD (N = 12). B. Left: Significant larger proportional area of astrocytes in the CC compared to the VC (Mann-Whitney-U test; p < .01) and in the DG compared to VC (Mann-Whitney-U test; p < .01) in ApoE$^{-/-}$ mice under SD (N = 9). Right: Significantly larger proportional area of astrocytes in the CC compared to the VC (Mann-Whitney-U test; p < .01) and in the DG compared to the VC (Mann-Whitney-U test; p < .01) in ApoE$^{-/-}$ mice under HCD (N = 12). Abbreviations: standard diet (SD), high cholesterol diet (HCD), corpus callosum (CC), dentate gyrus (DG), visual cortex (VC).*

4.1.3. PACAP$^{-/-}$/ApoE$^{-/-}$ mice

In PACAP$^{-/-}$/ApoE$^{-/-}$ mice under SD there was a significantly higher number of astrocytes in the CC as well as the DG compared to the VC. There was no statistically significant difference in the number of astrocytes in the CC as compared to the DG. Furthermore, the proportional area of astrocytes did not show any regional differences when fed an SD (*Figure 9*).

PACAP$^{-/-}$/ApoE$^{-/-}$ mice under HCD showed a significantly higher number of astrocytes in the CC as well as the DG compared to the VC. In the proportional area of GFAP-stained astrocyte profiles a regional difference was seen when comparing DG and VC. No other comparison yielded significant differences (*Figure 9*).

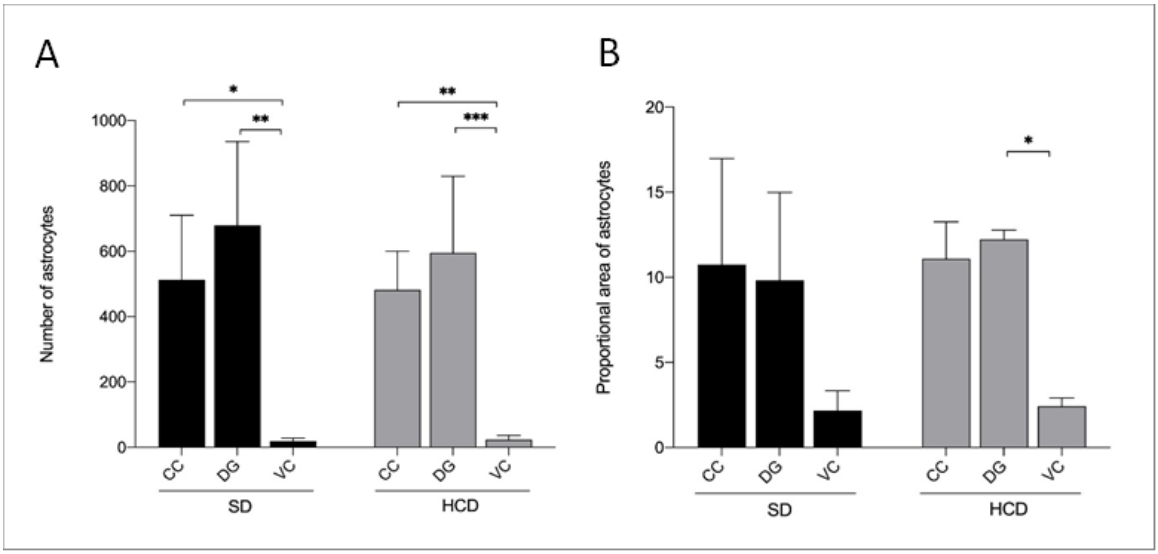

Figure 9. Regional differences in the number of astrocytes (A) and the proportional area of astrocytes (B) in PACAP$^{-/-}$/ApoE$^{-/-}$ mice under SD and HCD*. A. Left: Significantly larger number of astrocytes in the CC compared to the VC (Mann-Whitney-U test; p < .05) as well as in the DG compared to the VC (Mann-Whitney-U test; p < .01) in PACAP$^{-/-}$/ApoE$^{-/-}$ mice under SD (N = 12). Right: Significantly larger number of astrocytes in the CC compared to the VC (Mann-Whitney-U test; p < .01) and in the DG compared to the VC (Mann-Whitney-U test; p < .001) in PACAP$^{-/-}$/ApoE$^{-/-}$ mice under HCD (N = 12). B. Left: No significant regional differences in the proportional area of astrocytes in PACAP$^{-/-}$/ApoE$^{-/-}$ mice under SD (N = 12). Right: Significantly larger proportional area of astrocytes in the DG compared to the VC (Mann-Whitney-U test; p < .05) in PACAP$^{-/-}$/ApoE$^{-/-}$ mice under HCD (N = 12). Abbreviations: standard diet (SD), high cholesterol diet (HCD), corpus callosum (CC), dentate gyrus (DG), visual cortex (VC).*

4.1.4. PAC1$^{-/-}$/ApoE$^{-/-}$ mice

Under SD there was a significantly higher number of astrocytes in the CC compared to the VC and in the DG compared to the VC. No significant difference was found when comparing the CC and the DG. No regional differences in the proportional area of astrocytes was observed when fed an SD (*Figure 10*).

Under HCD significant differences in the number of astrocytes were observed in the CC as well as in the DG compared to the VC. No significant differences were found when comparing the CC and the DG. PAC1$^{-/-}$/ApoE$^{-/-}$ mice fed an HCD showed regional differences in the proportional area of astrocytes when comparing the VC to the CC and the DG. But there were no regional differences in the proportional area of astrocytes when comparing the CC and the fDG (*Figure 10*).

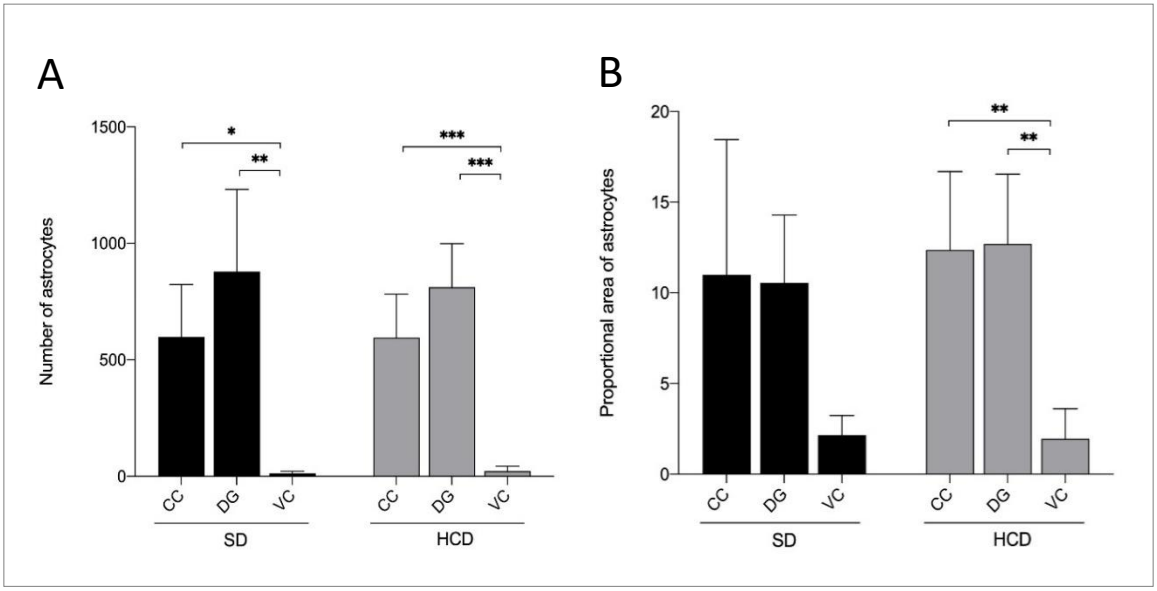

Figure 10. Regional differences in the number of astrocytes (A) and the proportional area of astrocytes (B) in PAC1$^{-/-}$/ApoE$^{-/-}$ mice under SD and HCD. *A. Left: Significantly larger number of astrocytes in the CC compared to the VC (Mann-Whitney-U test; p < .05) and in the DG compared to the VC (Mann-Whitney-U test; p < .01) in PAC1$^{-/-}$/ApoE$^{-/-}$ mice under SD (N = 12). Right: Significantly larger number of astrocytes in the CC compared to the VC (Mann-Whitney-U test; p < .001) and in the DG compared to the VC (Mann-Whitney-U test; p < .001) in PAC1$^{-/-}$/ApoE$^{-/-}$ mice under HCD (N = 12). B. Left: No significant regional differences in the proportional area of astrocytes in PAC1$^{-/-}$/ApoE$^{-/-}$ mice under SD (N = 12). Right: Significantly larger proportional area of astrocytes in the CC compared to the VC (Mann-Whitney-U test; p < .01) and in the DG compared to the VC (Mann-Whitney-U test; p < .01) in PAC1$^{-/-}$/ApoE$^{-/-}$ mice under HCD (N = 12). Abbreviations: standard diet (SD), high cholesterol diet (HCD), corpus callosum (CC), dentate gyrus (DG), visual cortex (VC).*

4.2. Astrocyte signatures are not influenced by genetic knockouts in mice fed an SD or an HCD

In mice fed an SD none of the two investigated astrocyte signatures (number of astrocytes and proportional area of astrocytes) differed significantly between wildtype and ApoE$^{-/-}$ mice. Likewise, neither PACAP-deficiency nor PAC1-deficiency in ApoE$^{-/-}$ mice significantly influenced astrocyte signatures as compared to the wildtype. No significant differences were revealed by pairwise comparisons of the four genotypes either. All comparisons were conducted in consideration of the investigated brain region (CC, DG and VC).

In mice fed an HCD the same results were seen. No significant differences were observed by pairwise comparisons of the four genotypes (WT, ApoE$^{-/-}$, PACAP$^{-/-}$

/ApoE$^{-/-}$ and PAC1$^{-/-}$/ApoE$^{-/-}$). No significant results were obtained in all three investigated brain regions (CC, DG and VC).

4.3. High cholesterol diet increases the proportional area of astrocytes in the dentate gyrus of wildtype mice as compared to mice under an SD, but has no effect on ApoE$^{-/-}$, PACAP$^{-/-}$/ApoE$^{-/-}$ and PAC1$^{-/-}$/ApoE$^{-/-}$ mice

When comparing SD fed WT mice to HCD fed WT mice there was a selective influence on astrocyte signatures. The selective region-specific increase in the dentate gyrus of HCD fed WT mice was in the proportional area of astrocytes while no influence was exhibited in the number of astrocytes. Besides, no effect was seen in the CC or the VC. Furthermore, no influence was seen in ApoE$^{-/-}$, PACAP$^{-/-}$/ApoE$^{-/-}$ and PAC1$^{-/-}$/ApoE$^{-/-}$ mice fed an HCD as compared to the same genotype group fed an SD. No significant results were obtained in both astrocyte signatures and in all investigated brain regions (CC, DG and VC) (shown in *Figure 11* and summarized in *Table 8* and *Table 9* in the *Appendix)*.

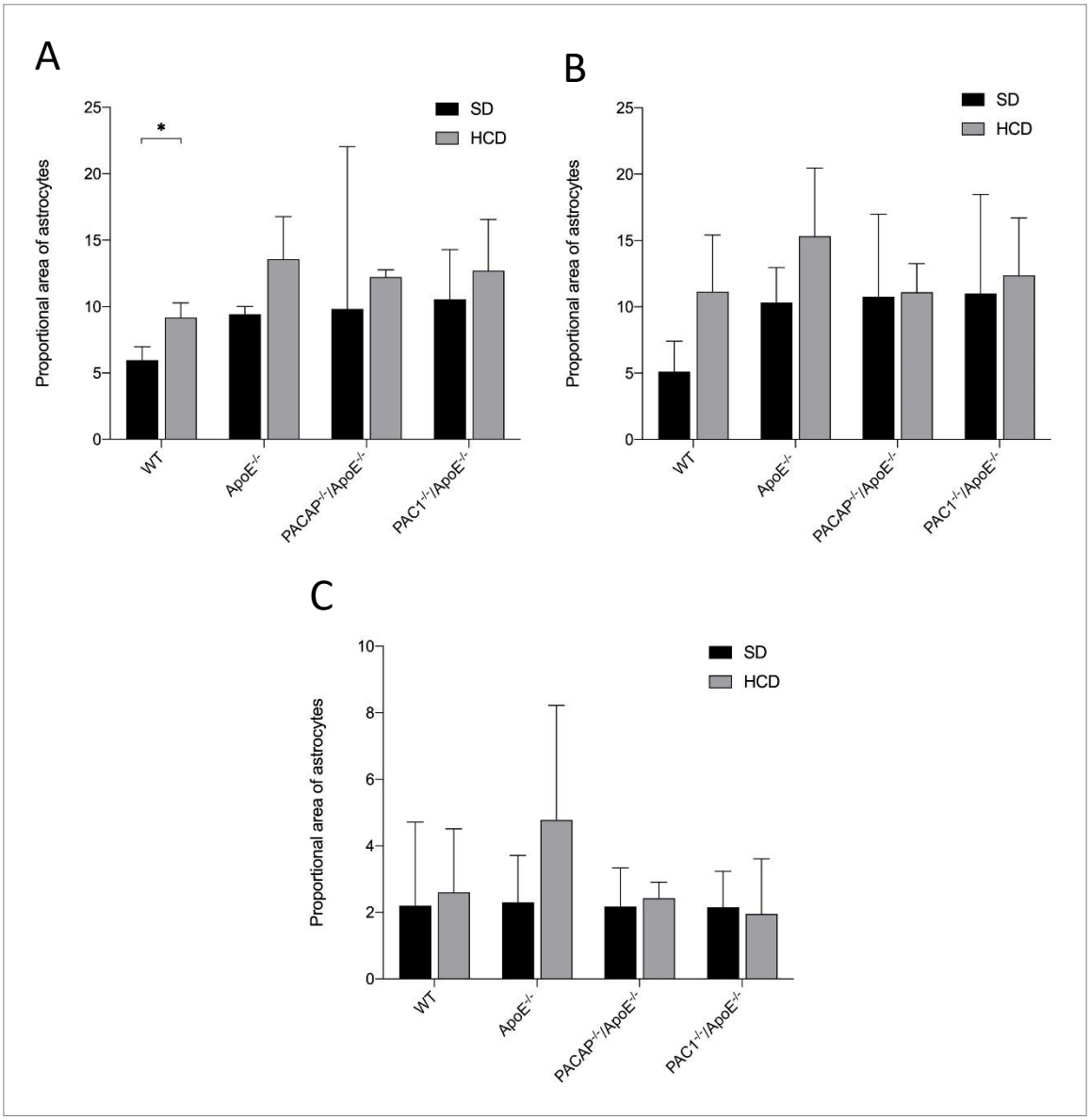

Figure 11. Effect of high cholesterol diet on the proportional area of astrocytes in the dentate gyrus (A), the corpus callosum (B) and the visual cortex (C). *A: HCD led to a significant increase in the proportional area of astrocytes in wildtype mice (Mann-Whitney-U test; p < .05; N = 7). No significant differences were seen between the diet groups in ApoE$^{-/-}$ (N = 7), PACAP$^{-/-}$/ApoE$^{-/-}$ (N = 8) and PAC1$^{-/-}$/ApoE$^{-/-}$ mice (N = 8). B and C: No significant differences between SD and HCD in the four genotypes (B and C: in WT and ApoE$^{-/-}$; N = 7; in PACAP$^{-/-}$/ApoE$^{-/-}$ and PAC1$^{-/-}$/ApoE$^{-/-}$; N = 8)). Abbreviations: standard diet (SD), high cholesterol diet (HCD), corpus callosum (CC), dentate gyrus (DG), visual cortex (VC).*

5. Discussion

The present study is the first to investigate the effect of a PACAP-deficiency and PAC1-deficiency in ApoE$^{-/-}$ mice on astrocyte signatures (number of astrocytes and proportional area of astrocytes) under SD and HCD. We aimed at evaluating the modulatory role of ApoE, PACAP and PAC1 on atherosclerotic processes in the periphery and how it effects astrocyte signatures in three different brain regions (namely corpus callosum, dentate gyrus and visual cortex).

5.1. High cholesterol diet associated increases in the proportional area of astrocytes are restricted to the dentate gyrus of wildtype mice and not seen in ApoE$^{-/-}$ mice

The key finding of our research is that an HCD led to a significant increase in the proportional area of GFAP-stained astrocytes in the DG of WT compared with WT mice fed an SD (*Figure 11*). In contrast, an HCD intake did not significantly influence the number of astrocytes. No significant differences were found between ApoE-deficient mice fed an HCD and an SD. Besides, the effect could neither be found in the CC nor in the VC. It is unclear why the effect of an HCD could only be found in the DG, however, the DG is a brain region extremely vulnerable to neuroinflammation and neurodegeneration (Abbott & Nigussie, 2020; Lana et al., 2017) and might thus have responded more strongly to the increase in cholesterol intake.

A possible explanation might be, the effect of the GFAP-stained astrocyte reaction is not directly caused by an HCD but indirectly through metabolic stress caused by an HCD. If this is the case, metabolic stress seems to be independent of the ApoE-knockout as it can only be seen in WT mice. The ApoE-knockout mice would then appear to be protected from astrocytic growth potentially because of the lack of an HCD mediator. This condition might work differently peripherally than centrally, as ApoE-expression can function differently in the brain than in the periphery. Whether this GFAP-stained astrocyte reaction has positive or negative effects cannot be said with certainty since astrocytes can have both pathological and neuroprotective effects.

Per se, our key finding is in line with our expectations and in line with the literature. In the DG specifically, mice under an HCD were hypothesized to show an increase in astrocytic responses due to HCD-induced inflammatory processes (cf. Neustadt, 2006) as well as HCD-induced inhibition of compensatory mechanisms (cf. Janssen et al., 2016). Hypercholesterolemia can lead to oxidative stress (Prasad & Kalra, 1993), which might be a mediator of HCD-induced inflammation. As seen in many CNS pathologies, astrocytes become activated in response to inflammation (Pekny & Nilsson, 2005), change their morphology and release proinflammatory chemokines and cytokines, which decreases cell survival and causes a shift away from neurogenesis towards astrogliogenesis (Chen et al., 2016; Griffin, 2006; Sofroniew, 2015). Various studies have linked hypercholesterolemia and inflammation to atherosclerosis (Joossens, 1988; Kottke et al., 1988) since the expression of proinflammatory chemokines and cytokines characterizes early atherosclerotic changes (Libby, 2000; Tracy, 1997).

Surprisingly, in our study, the increase in cholesterol only seemed to affect the proportional area but not the *number* of astrocytes. Potentially, the recruitment of further astroglia to the DG would have followed further downstream in the neuroinflammatory cascade, as it seems unlikely to assume that HCD would affect astrocytic growth by increasing the proportional area of astrocytes whilst having no effect on the number of astrocytes. Further studies area necessary to investigate this hypothesis.

5.2. High cholesterol diet did not influence astrocyte signatures in PACAP- and PAC1- deficient ApoE$^{-/-}$ mice

When comparing SD fed with HCD fed double-knockout (PACAP$^{-/-}$/ApoE$^{-/-}$ and PAC1$^{-/-}$/ApoE$^{-/-}$) mice, another rather unexpected finding is that no effect on astrocyte signatures was seen. Hence, an additive effect of HCD, PACAP- and/or PAC1-deficiency, respectively, cannot be assumed at this point. Potentially, PACAP- and/or PAC1-deficiency in ApoE$^{-/-}$ mice already causes an increase in astroglial responses where the influence of diet is negligible, and therefore

differences might not be significant. However, it might also be that the metabolic stress caused by the HCD is not mediated through the knockouts, and therefore differences might not be significant. In addition, PACAP- and PAC1-deficient mice were always considered in combination with ApoE-deficiency. To circumvent the influence of ApoE-deficiency, $PACAP^{-/-}/ApoE^{+/+}$ and $PAC1^{-/-}/ApoE^{+/+}$ mice could also be added as a control group. This would allow the influence of PACAP and PAC1 on astrocyte signatures to be assessed more accurately. Further investigation with different experimental conditions is necessary to explore this possible explanation.

5.3. No impact of genotype on astrocyte signatures in either diet (SD and HCD)

Under SD, immunohistochemistry of the investigated mice brain slices did not reveal any effect of the genotypes on astrocyte signatures. Differences between the four genotypes (WT, $ApoE^{-/-}$, $PACAP^{-/-}/ApoE^{-/-}$, $PAC1^{-/-}/ApoE^{-/-}$) were neither observed in the number of astrocytes nor in the proportional area of GFAP-stained astrocytes, independent of the brain region (CC, DG, VD). Furthermore, pairwise comparisons of WT, $ApoE^{-/-}$, $PACAP^{-/-}/ApoE^{-/-}$, $PAC1^{-/-}/ApoE^{-/-}$ mice fed an HCD did also failed to reveal any changes in astrocyte signatures in any of the three investigated brain regions (CC, DG, VC). Notably, on a descriptive level, fewer astrocytes were counted in WT than in $ApoE^{-/-}$ mice, and the relationship might have reached statistical significance in a larger sample size and/or with an extended feeding time. This would have then been in line with the findings by Crisby et al. (2004). In their study, HCD induced a marked astrocyte proliferation but yielded similar astrocyte activation in ApoE-deficient mice as in WT mice (Crisby et al., 2004; Walker et al., 1997).

5.4. Brain region-specific differences in astrocyte signatures

The present study revealed significant differences in astrocyte signatures between the three investigated brain regions - the corpus callosum, the dentate gyrus and the visual cortex.

A significantly higher number of astrocytes was found in the DG compared to the VC in SD fed WT mice, and a significantly higher number of astrocytes was seen in the DG and CC compared to the VC in HCD fed WT mice (*Figure 7*). In ApoE$^{-/-}$ mice as well as in PACAP$^{-/-}$/ApoE$^{-/-}$ and PAC1$^{-/-}$/ApoE$^{-/-}$ mice, a significantly higher number of astrocytes was found in the DG and CC compared to the VC (*Figure 8, Figure 9, Figure 10*).

With regard to the proportional area of astrocytes, there were no significant differences between the brain regions in WT mice (*Figure 7*), however, in ApoE$^{-/-}$ mice the proportional area of GFAP-stained astrocytes was larger in the DG and CC compared to the VC in both diet groups (SD and HCD) (*Figure 8*). In PACAP$^{-/-}$/ApoE$^{-/-}$ mice under HCD, the proportional area of astrocytes was larger in the DG than in the VC (*Figure 9*), and in PAC1$^{-/-}$/ApoE$^{-/-}$ mice under HCD, both the DG and CC demonstrated larger proportional areas of astrocytes in comparison to the VC (*Figure 10*).

Although a comprehensive interpretation of the regional differences is difficult and more data is needed, previous research suggests a vast heterogeneity of astrocyte populations differing between brain regions, which is mainly due to differences in the levels of gene expression, e.g., of cytokines and growth factors (Schmidt Buosi et al., 2018). Critically, the level of basal GFAP-expression and alterations in GFAP expression, as well as the number of GFAP-positive cells, the type and stage of disease or injury depend on the brain region, which should be taken into account when drawing conclusions from our study (Kimelberg, 2004; Matias et al., 2019; Rodríguez et al., 2014). Region-specific astrocyte responses to injury have been demonstrated previously (e.g. Cragnolini et al., 2018). Notably, differences in astroglial response in the hippocampus compared to the cortex have been shown by Clarke et al. (2018), who found a larger number of upregulated reactive astrocyte genes in hippocampal astrocytes compared

with cortical astrocytes, which could potentially serve as an explanation for our findings.

5.5. Limitations and future directions

As mentioned above, one significant limitation of the study might have been the rather small sample size of 30 mice, divided into four genotypes and split again by diet, resulting in eight subsamples each comprising three to four mice (for details please refer to *Table 1*). In addition, the respective subgroups of mice were only fed with an HCD for twenty weeks, while other research groups have used longer feeding periods (e.g. Williams et al., 2002) to create an atherosclerotic mouse model in ApoE-deficient mice. Future research should therefore replicate the experiment using a larger sample size and an extended feeding time.

Although previous research has demonstrated the comparability of atherosclerotic lesions in the mice model and human atherosclerosis (Getz & Reardon, 2012; Meir & Leitersdorf, 2004), limitations must still be kept in mind when transferring knowledge from animal research to human medicine. While our results question the role of PACAP and PAC1 as a therapeutic target in the treatment of atherosclerosis-induced neuroinflammation, more research is needed to provide more solid evidence.

On a more technical level, recording various layer depths per brain region could have improved the quality of our data. Depending on the depth of cut, the astrocyte body is either completely visible, only partially visible, or only the foothills are visible. Future studies could use different cut depths and compare the results. A bias might have also resulted from obtaining slightly different brain layers from different mice. However, since this is not a systematic error and should have occurred in all subgroups equally randomly, statistically, this aspect should not have affected the findings.

As another limitation it should be mentioned that, although astrocytes have been counted by means of ImageJ, which is a state-of-the-art software, there is no standardized method of astrocyte counting, making the process prone to

measurement error. The difficulty with standardized counting of astrocytes lies in their individual form factor. As astrocytes are star-shaped with versatile branching structures, automated counting is rather difficult, compared to clearly defined cells. To overcome the problem and to make data comparable at least within the present study, all images were processed in the same way. Additionally, the images were processed twice, once manually and once automatically, with excellent inter-rating reliabilities (r = .94). Moreover, with the additional assessment of the proportional area of GFAP-stained astrocytes, we have complemented and improved our research design.

This study was limited to staining astrocytes using GFAP, since it is state of the art as an astrocyte marker (Escartin et al., 2021). However, GFAP does not allow differentiation between astrocyte subgroups A1 and A2. For this purpose, the markers C3 (A1) and EMP1 (A2) (Khodadadei et al., 2021) should be considered more closely. This would possibly allow conclusions about neuroprotective or neurotoxic processes through the astrocyte signatures in further studies.

Future experiments should also include the additional investigation of a proliferation marker such as Ki67 and/or study astroglial-neuronal-communication, e.g. by means of doublecortin. Importantly, the influence of PACAP- and PAC1-deficiency in ApoE-deficient mice under standard or high cholesterol diet should also be investigated in microglia, as they are, effectively, the resident immune cells of the brain, play a key role in neuroinflammation and communicate with astrocytes and neurons (Bazan et al., 2012).

5.6. Conclusion

In the present study we have shown that a high cholesterol diet had a selective, region-specific influence on astrocytes signatures, namely an increase in the proportional area of GFAP-stained astrocytes in the DG of WT mice. Contrary to our hypothesis, ApoE-deficiency alone or combined with PACAP- or PAC1-deficiency under SD or HCD did not lead to differences in astrocyte signatures. Therefore we question the role of PACAP and PAC1 in the pathophysiology of atherosclerosis-associated neuroinflammation in the brain. Moreover, we found regional differences in astrocyte signatures with the DG and CC showing stronger

astroglial response than the VC. Future studies are needed to replicate the experiment and confirm our findings.

6. Abstract

6.1. Abstract (English)

Given the immunoregulatory roles of pituitary adenylate cyclase-activating polypeptide (PACAP) in general, the effects of the polypeptide on astroglia and the recent evidence showing that astroglial response profiles are affected by apolipoprotein E-(ApoE)-deficiency, the aim of the present study was to test whether PACAP-deficiency and/or a deficiency in its receptor PAC1 in ApoE-knockout mice determine astroglial response signatures under standard diet or under high cholesterol diet.

After immunohistochemical staining for the astrocyte marker glial fibrillary acidic protein (GFAP), astrocyte numbers and the proportional area of astrocytes were analyzed in the dentate gyrus, corpus callosum and visual cortex of mice with four different genotypes, including wildtype mice (WT), ApoE-single-knockout mice ($ApoE^{-/-}$), PACAP and ApoE double-knockout mice ($PACAP^{-/-}/ApoE^{-/-}$) as well as PAC1 and ApoE double-knockout mice ($PAC1^{-/-}/ApoE^{-/-}$) which had been previously fed with a standard diet or a high cholesterol diet.

Compared to a standard diet (SD), a high cholesterol diet (HCD) led to a significant increase in the proportional area of astrocytes in the dentate gyrus of wildtype mice, but not in the number of astrocytes. The effect was found neither in the corpus callosum nor in the visual cortex, although generally, significant regional differences in astroglial signatures were observed. Notably, there was no significant effect of the genotype on astrocyte responses in SD or HCD.

Although replication is needed to confirm the results, our study provides further evidence of a cholesterol-induced astroglial response in the dentate gyrus and questions the role of PACAP and PAC1 in the pathophysiology of atherosclerosis-associated neuroinflammation in the brain.

6.2. Zusammenfassung (Deutsch)

In Anbetracht der immunregulatorischen Rolle von PACAP (Pituitary Adenylate Cylase-Activating Polypeptide), der Auswirkungen des Polypeptids auf Astrozyten sowie jüngster Befunde, die zeigen, dass Apolipoprotein E-(ApoE)-Defizienz das Reaktionsverhalten von Astrozyten beeinflusst, war es das Ziel der vorliegenden Studie, zu testen, wie sich ein PACAP- und/oder ein Mangel seines Rezeptors PAC1 in ApoE-Knockout-Mäusen unter einer Standarddiät verglichen mit einer cholesterinreichen Diät auswirkt.

Nach immunohistologischer Färbung mittels des Astrozytenmarkers saures Gliafaserprotein (GFAP) wurde die Astrozytenanzahl sowie die proportionale Fläche der Astrozyten im Gyrus dentatus, Corpus callosum sowie im visuellen Cortex von Mäusen vierer Genotypen analysiert, einschließlich Wildtypmäuse (WT), ApoE-Single-Knockout Mäuse ($ApoE^{-/-}$), PACAP und ApoE Double-Knockout Mäuse ($PACAP^{-/-}/ApoE^{-/-}$) sowie PAC1 und ApoE Double-Knockout Mäuse ($PAC1^{-/-}/ApoE^{-/-}$), die zuvor mit einer cholesterinreichen oder einer Standarddiät gefüttert wurden.

Im Vergleich zur Standarddiät (SD) führte eine cholesterinreiche Diät (HCD) im Gyrus dentatus von Wildtypmäusen zu einer signifikanten Zunahme der proportionalen Fläche von Astrozyten, nicht jedoch der Astrozytenanzahl. Der Effekt konnte weder im Corpus callosum, noch im visuellen Cortex gefunden werden, obwohl allgemeine regionale Unterschiede in den Astrozytensignaturen beobachtet wurden. Allerdings wurde kein signifikanter Effekt des Genotyps auf die Astrozytenreaktion festgestellt.

Auch wenn Replikationen notwendig sind, um die Ergebnisse zu bestätigen, ergeben sich aus unserer Studie weitere Hinweise auf Cholesterin-induzierte Astrozytenreaktionen im Gyrus dentatus. Zudem stellen die Ergebnisse eine mögliche Rolle von PACAP und PAC1 als therapeutische Zielmoleküle bei der Behandlung von Atherosklerose-verursachter Neuroinflammation in Frage.

7. References

Abad, C., Gomariz, R., & Waschek, J. (2006). Neuropeptide Mimetics and Antagonists in the Treatment of Inflammatory Disease: Focus on VIP and PACAP. *Current Topics in Medicinal Chemistry*, *6*(2), 151–163. https://doi.org/10.2174/156802606775270288

Abbott, L. C., & Nigussie, F. (2020). Adult neurogenesis in the mammalian dentate gyrus. *Journal of Veterinary Medicine Series C: Anatomia Histologia Embryologia*, *49*(1), 3–16. https://doi.org/10.1111/ahe.12496

Aimone, J. B., Wiles, J., & Gage, F. H. (2006). Potential role for adult neurogenesis in the encoding of time in new memories. *Nature Neuroscience*, *9*(6), 723–727. https://doi.org/10.1038/nn1707

Amaral, D. G., Scharfman, H. E., & Lavenex, P. (2007). The dentate gyrus: fundamental neuroanatomical organization (dentate gyrus for dummies). *Progress in Brain Research*, *163*, 3–22. https://doi.org/10.1016/S0079-6123(07)63001-5

Amor, S., Puentes, F., Baker, D., & Van Der Valk, P. (2010). Inflammation in neurodegenerative diseases. *Immunology*, *129*(2), 154–169. https://doi.org/10.1111/j.1365-2567.2009.03225.x

Bähr, M., & Frotscher, M. (2003). *Duus' Neurologisch-topische Diagnostik* (8th ed.). Georg Thieme Verlag.

Bandopadhyay, R., Liu, J. Y. W., Sisodiya, S. M., & Thom, M. (2014). A comparative study of the dentate gyrus in hippocampal sclerosis in epilepsy and dementia. *Neuropathology and Applied Neurobiology*, *40*(2), 177–190. https://doi.org/10.1111/nan.12087

Baxter, P. S., Martel, M. A., McMahon, A., Kind, P. C., & Hardingham, G. E. (2011). Pituitary adenylate cyclase-activating peptide induces long-lasting neuroprotection through the induction of activity-dependent signaling via the cyclic AMP response element-binding protein-regulated transcription co-activator 1. *Journal of Neurochemistry*, *118*(3), 365–378. https://doi.org/10.1111/j.1471-4159.2011.07330.x

Bazan, N. G., Halabi, A., Ertel, M., & Petasis, N. A. (2012). Neuroinflammation. In *Basic Neurochemistry* (pp. 610–620). Elsevier. https://doi.org/10.1016/B978-0-12-374947-5.00034-1

Bertrand, G., Puech, R., Maisonnasse, Y., Bockaert, J., & Loubatières-Mariani, M. M. (1996). Comparative effects of PACAP and VIP on pancreatic endocrine secretions and vascular resistance in rat. *British Journal of Pharmacology*, *117*(4), 764–770. https://doi.org/10.1111/j.1476-5381.1996.tb15256.x

Bonaterra, G. A., Zügel, S., Thogersen, J., Walter, S. A., Haberkorn, U., Strelau, J., & Kinscherf, R. (2012). Growth differentiation factor-15 deficiency inhibits atherosclerosis progression by regulating interleukin-6-dependent inflammatory response to vascular injury. *Journal of the American Heart Association*, *1*(6). https://doi.org/10.1161/JAHA.112.002550

Bondan, E. F., Cardoso, C. V., Martins, M. D. F. M., & Otton, R. (2019). Memory impairments and increased GFAP expression in hippocampal astrocytes following hypercaloric diet in rats. *Arquivos de Neuro-Psiquiatria*, *77*(9), 601–608. https://doi.org/10.1590/0004-282X20190091

Boyles, J. K., Pitas, R. E., Wilson, E., Mahley, R. W., & Taylor, J. M. (1985). Apolipoprotein E associated with astrocytic glia of the central nervous system and with nonmyelinating glia of the peripheral nervous system. *Journal of Clinical Investigation*, *76*(4), 1501–1513. https://doi.org/10.1172/JCI112130

Buckman, L. B., Thompson, M. M., Moreno, H. N., & Ellacott, K. L. J. (2013). Regional astrogliosis in the mouse hypothalamus in response to obesity. *Journal of Comparative Neurology*, *521*(6), 1322–1333. https://doi.org/10.1002/cne.23233

Buosi, A. S., Matias, I., Araujo, A. P. B., Batista, C., & Gomes, F. C. A. (2018). Heterogeneity in Synaptogenic Profile of Astrocytes from Different Brain Regions. *Molecular Neurobiology*, *55*(1), 751–762. https://doi.org/10.1007/s12035-016-0343-z

Buschmann, J. P., Berger, K., Awad, H., Clarner, T., Beyer, C., & Kipp, M. (2012).

Inflammatory Response and Chemokine Expression in the White Matter Corpus Callosum and Gray Matter Cortex Region During Cuprizone-Induced Demyelination. *Journal of Molecular Neuroscience*, *48*(1), 66–76. https://doi.org/10.1007/s12031-012-9773-x

Cerami, C., & Perani, D. (2015). Imaging Neuroinflammation in Ischemic Stroke and in the Atherosclerotic Vascular Disease. *Current Vascular Pharmacology*, *13*(2), 218–222. https://doi.org/10.2174/15701611113116660168

Chait, A., & Bornfeldt, K. E. (2009). Diabetes and atherosclerosis: Is there a role for hyperglycemia? *Journal of Lipid Research*, *50*(SUPPL.), 335–339. https://doi.org/10.1194/jlr.R800059-JLR200

Chang, Q. (1997). [Experimental study of the effects of pituitary adenylate cyclase-activating polypeptide (PACAP) and its mechanism on the vascular cell components--the possible relationship between PACAP and atherosclerosis]. *Sheng Li Ke Xue Jin Zhan [Progress in Physiology]*, *28*(2), 132–135. http://www.ncbi.nlm.nih.gov/pubmed/11038706

Charleston, J. S., Bolender, R. P., Mottet, N. K., Body, R. L., Vahter, M. F., & Burbacher, T. M. (1994). Increases in the number of reactive glia in the visual cortex of macaca fascicularis following subclinical long-term methyl mercury exposure. In *Toxicology and Applied Pharmacology* (Vol. 129, Issue 2, pp. 196–206). https://doi.org/10.1006/taap.1994.1244

Chen, W. W., Zhang, X., & Huang, W. J. (2016). Role of neuroinflammation in neurodegenerative diseases (Review). *Molecular Medicine Reports*, *13*(4), 3391–3396. https://doi.org/10.3892/mmr.2016.4948

Chrysikopoulos, H., Andreou, J., Roussakis, A., & Pappas, J. (1997). Infarction of the corpus callosum: Computed tomography and magnetic resonance imaging. *European Journal of Radiology*, *25*(1), 2–8. https://doi.org/10.1016/S0720-048X(96)01155-2

Clarke, L. E., Liddelow, S. A., Chakraborty, C., Münch, A. E., Heiman, M., & Barres, B. A. (2018). Normal aging induces A1-like astrocyte reactivity. *Proceedings of the National Academy of Sciences*, *115*(8), E1896–E1905.

https://doi.org/10.1073/pnas.1800165115

Cragnolini, A. B., Montenegro, G., Friedman, W. J., & Mascó, D. H. (2018). Brain-region specific responses of astrocytes to an in vitro injury and neurotrophins. *Molecular and Cellular Neuroscience*, *88*, 240–248. https://doi.org/10.1016/j.mcn.2018.02.007

Crisby, M., Rahman, S. M. A., Sylvén, C., Winblad, B., & Schultzberg, M. (2004). Effects of high cholesterol diet on gliosis in apolipoprotein E knockout mice: Implications for Alzheimer's disease and stroke. *Neuroscience Letters*, *369*(2), 87–92. https://doi.org/10.1016/j.neulet.2004.05.057

Cui, J. G., Hill, J. M., Zhao, Y., & Lukiw, W. J. (2007). Expression of inflammatory genes in the primary visual cortex of late-stage Alzheimer's disease. *NeuroReport*, *18*(2), 115–119. https://doi.org/10.1097/WNR.0b013e32801198bc

D., C., J., R., & J., P. (2005). Effect of apolipoprotein E deficiency on reactive sprouting in the dentate gyrus of the hippocampus following entorhinal cortex lesion: Role of the astroglial response. *Experimental Neurology*, *194*(1), 31–42. http://www.embase.com/search/results?subaction=viewrecord&from=export&id=L40719742%0Ahttp://dx.doi.org/10.1016/j.expneurol.2005.01.016

Davignon, J. (2005). Apolipoprotein E and Atherosclerosis. *Arteriosclerosis, Thrombosis, and Vascular Biology*, *25*(2), 267–269. https://doi.org/10.1161/01.ATV.0000154570.50696.2c

De La Monte, S. M., Longato, L., Tong, M., & Wands, J. R. (2009). Insulin resistance and neurodegeneration: Roles of obesity, type 2 diabetes mellitus and non-alcoholic steatohepatitis. *Current Opinion in Investigational Drugs*, *10*(10), 1049–1060.

Dejda, A., Sokołowska, P., & Nowak, J. Z. (2005). Neuroprotective potential of three neuropeptides PACAP, VIP and PHI. *Pharmacological Reports*, *57*(3), 307–320.

Devaney, K. O., & Johnson, H. A. (1980). Neuron loss in the aging visual cortex of man. *Journals of Gerontology*, *35*(6), 836–841.

https://doi.org/10.1093/geronj/35.6.836

Dietemann, J. L., Beigelman, C., Rumbach, L., Vouge, M., Tajahmady, T., Faubert, C., Jeung, M. Y., & Wackenheim, A. (1988). Multiple sclerosis and corpus callosum atrophy: Relationship of MRI findings to clinical data. *Neuroradiology*, *30*(6), 478–480. https://doi.org/10.1007/BF00339686

Emini Veseli, B., Perrotta, P., De Meyer, G. R. A., Roth, L., Van der Donckt, C., Martinet, W., & De Meyer, G. R. Y. (2017). Animal models of atherosclerosis. *European Journal of Pharmacology*, *816*, 3–13. https://doi.org/10.1016/j.ejphar.2017.05.010

Escartin, C., Galea, E., Lakatos, A., O'Callaghan, J. P., Petzold, G. C., Serrano-Pozo, A., Steinhäuser, C., Volterra, A., Carmignoto, G., Agarwal, A., Allen, N. J., Araque, A., Barbeito, L., Barzilai, A., Bergles, D. E., Bonvento, G., Butt, A. M., Chen, W.-T., Cohen-Salmon, M., … Verkhratsky, A. (2021). Reactive astrocyte nomenclature, definitions, and future directions. *Nature Neuroscience*, *24*(3), 312–325. https://doi.org/10.1038/s41593-020-00783-4

Falk, E. (2006). Pathogenesis of Atherosclerosis. *Journal of the American College of Cardiology*, *47*(8 SUPPL.), 6. https://doi.org/10.1016/j.jacc.2005.09.068

Fan, Y.-Y., & Huo, J. (2021). A1/A2 astrocytes in central nervous system injuries and diseases: Angels or devils? *Neurochemistry International*, *148*, 105080. https://doi.org/10.1016/j.neuint.2021.105080

Filipsson, K., Tornøe, K., Holst, J., & Ahre, B. (2015). *Stimulates Insulin and Glucagon Secretion in Humans* *. *82*(9), 3093–3098.

Fitsiori, A., Nguyen, D., Karentzos, A., Delavelle, J., & Vargas, M. I. (2011). The corpus callosum: White matter or terra incognita. *British Journal of Radiology*, *84*(997), 5–18. https://doi.org/10.1259/bjr/21946513

Gasz, B., Rácz, B., Roth, E., Borsiczky, B., Ferencz, A., Tamás, A., Cserepes, B., Lubics, A., Gallyas, F., Tóth, G., Lengvári, I., & Reglodi, D. (2006). Pituitary adenylate cyclase activating polypeptide protects cardiomyocytes against oxidative stress-induced apoptosis. *Peptides*, *27*(1), 87–94. https://doi.org/10.1016/j.peptides.2005.06.022

Getz, G. S., & Reardon, C. A. (2012). Animal Models of Atherosclerosis. *Arteriosclerosis, Thrombosis, and Vascular Biology*, *32*(5), 1104–1115. https://doi.org/10.1161/ATVBAHA.111.237693

Glass, C. K., & Witztum, J. L. (2001). Atherosclerosis: The Road Ahead. *Cell*, *104*(4), 503–516.

Goldstein, A., Covington, B. P., Mahabadi, N., & Mesfin, F. B. (2022). *Neuroanatomy , Corpus Callosum*. 20894.

Gonzalez-Perez, O., Quiñones-Hinojosa, A., & Garcia-Verdugo, J. M. (2010). Immunological control of adult neural stem cells. *Autoimmune Diseases: Symptoms, Diagnosis and Treatment*, *5*(1), 303–316.

Greenow, K., Pearce, N. J., & Ramji, D. P. (2005). The key role of apolipoprotein e in atherosclerosis. *Journal of Molecular Medicine*, *83*(5), 329–342. https://doi.org/10.1007/s00109-004-0631-3

Griffin, W. S. T. (2006). Inflammation and neurodegenerative diseases. *American Journal of Clinical Nutrition*, *83*(2), 470–474. https://doi.org/10.1093/ajcn/83.2.470s

Groh, L., Keating, S. T., Joosten, L. A. B., Netea, M. G., & Riksen, N. P. (2018). Monocyte and macrophage immunometabolism in atherosclerosis. *Seminars in Immunopathology*, *40*(2), 203–214. https://doi.org/10.1007/s00281-017-0656-7

Grundy, S. M., Brewer, H. B., Cleeman, J. I., Smith, S. C., & Lenfant, C. (2004). Definition of Metabolic Syndrome. *Circulation*, *109*(3), 433–438. https://doi.org/10.1161/01.cir.0000111245.75752.c6

Hamelink, C., Tjurmina, O., Damadzic, R., Young, W. S., Weihe, E., Lee, H. W., & Eiden, L. E. (2002). Pituitary adenylate cyclase-activating polypeptide is a sympathoadrenal neurotransmitter involved in catecholamine regulation and glucohomeostasis. *Proceedings of the National Academy of Sciences of the United States of America*, *99*(1), 461–466. https://doi.org/10.1073/pnas.012608999

Han, P., Caselli, R. J., Baxter, L., Serrano, G., Yin, J., Beach, T. G., Reiman, E. M., & Shi, J. (2015). Association of Pituitary Adenylate Cyclase-Activating

Polypeptide with Cognitive Decline in Mild Cognitive Impairment Due to Alzheimer Disease. *JAMA Neurology*, *72*(3), 1–12. https://doi.org/10.4049/jimmunol.1801473.The

Harmar, A. J., Arimura, A., Gozes, I., Journot, L., Laburthe, M., Pisegna, J. R., Rawlings, S. R., Robberecht, P., Said, S. I., Sreedharan, S. P., Wank, S. A., & Waschek, J. A. (1998). International Union of Pharmacology. XVIII. Nomenclature of receptors for vasoactive intestinal peptide and pituitary adenylate cyclase-activating polypeptide. *Pharmacological Reviews*, *50*(2), 265–270. http://www.ncbi.nlm.nih.gov/pubmed/9647867

Hattingen, E., Nichtweiss, M., Blasel, S., Zanella, F. E., & Weidauer, S. (2010). Corpus callosum. Landmark of the origin of cerebral diseases. *Der Radiologe*, *50*(2), 152–164. https://doi.org/10.1007/s00117-009-1945-5

Hennes, M., Lombaert, N., Wahis, J., Van den Haute, C., Holt, M. G., & Arckens, L. (2020). Astrocytes shape the plastic response of adult cortical neurons to vision loss. *Glia*, *68*(10), 2102–2118. https://doi.org/10.1002/glia.23830

Hill, J. M., Dua, P., Clement, C., & Lukiw, W. J. (2014). Opinion: An evaluation of progressive amyloidogenic and pro-inflammatory change in the primary visual cortex and retina in Alzheimer's disease (AD). *Frontiers in Neuroscience*, *8*(OCT), 8–11. https://doi.org/10.3389/fnins.2014.00347

Huang, Y., & Mahley, R. W. (2014). Apolipoprotein E: Structure and function in lipid metabolism, neurobiology, and Alzheimer's diseases. *Neurobiology of Disease*, *72*, 3–12. https://doi.org/10.1016/j.nbd.2014.08.025

Huff, T., Mahabadi, N., & Tadi, P. (2022). Neuroanatomy, Visual Cortex. In *StatPearls*. http://www.ncbi.nlm.nih.gov/pubmed/29494110

Huttmann, K., Sadgrove, M., Wallraff, A., Hinterkeuser, S., Kirchhoff, F., Steinhauser, C., & Gray, W. P. (2003). Seizures preferentially stimulate proliferation of radial glia-like astrocytes in the adult dentate gyrus: functional and immunocytochemical analysis. *European Journal of Neuroscience*, *18*(10), 2769–2778. https://doi.org/10.1111/j.1460-9568.2003.03002.x

Jackson, R. J., Meltzer, J. C., Nguyen, H., Commins, C., Bennett, R. E., Hudry, E., & Hyman, B. T. (2021). APOE4 derived from astrocytes leads to blood–

brain barrier impairment. *Brain*. https://doi.org/10.1093/brain/awab478

Jamen, F., Persson, K., Bertrand, G., Rodriguez-Henche, N., Puech, R., Bockaert, J., Ahrén, B., & Brabet, P. (2000). PAC1 receptor-deficient mice display impaired insulinotropic response to glucose and reduced glucose tolerance. *Journal of Clinical Investigation*, *105*(9), 1307–1315. https://doi.org/10.1172/JCI9387

Janssen, C. I. F., Jansen, D., Mutsaers, M. P. C., Dederen, P. J. W. C., Geenen, B., Mulder, M. T., & Kiliaan Kiliaan, A. J. (2016). The effect of a high-fat diet on brain plasticity, inflammation and cognition in female ApoE4-knockin and ApoE-knockout mice. *PLoS ONE*, *11*(5), 1–16. https://doi.org/10.1371/journal.pone.0155307

Joossens, J. V. (1988). Mechanisms of hypercholesterolemia and atherosclerosis. *Acta Cardiologica. Supplementum*, *29*, 63–83. http://www.ncbi.nlm.nih.gov/pubmed/3389027

Khodadadei, F., Arshad, R., Morales, D. M., Gluski, J., Marupudi, N. I., McAllister, J. P., Limbrick, D. D., & Harris, C. A. (2021). *The Effect of A1/A2 Reactive Astrocyte Expression on Hydrocephalus Shunt Failure*. 2021.11.04.467357. https://www.biorxiv.org/content/10.1101/2021.11.04.467357v1%0Ahttps://www.biorxiv.org/content/10.1101/2021.11.04.467357v1.abstract

Kimelberg, H. K. (2004). The problem of astrocyte identity. *Neurochemistry International*, *45*(2–3), 191–202. https://doi.org/10.1016/j.neuint.2003.08.015

Klinteberg, K. A., Karlsson, S., & Ahrén, B. (1996). Signaling mechanisms underlying the insulinotropic effect of pituitary adenylate cyclase-activating polypeptide in HIT-T15 cells. *Endocrinology*, *137*(7), 2791–2798. https://doi.org/10.1210/endo.137.7.8770899

Kohman, R. A., & Rhodes, J. S. (2013). Neurogenesis, inflammation and behavior. *Brain, Behavior, and Immunity*, *27*, 22–32. https://doi.org/10.1016/j.bbi.2012.09.003

Kottke, B. A., Pineda, A. A., Case, M. T., Orsuzar, A. M., & Brzys, K. A. (1988). Hypercholesterolemia and atherosclerosis: Present and future therapy

including LDL-apheresis. *Journal of Clinical Apheresis*, *4*(1), 35–46. https://doi.org/10.1002/jca.2920040108

Koutseff, A., Mittelhaeuser, C., Essabri, K., Auwerx, J., & Meziane, H. (2014). Impact of the apolipoprotein e polymorphism, age and sex on neurogenesis in mice: Pathophysiological relevance for Alzheimer's disease? *Brain Research*, *1542*(5), 32–40. https://doi.org/10.1016/j.brainres.2013.10.003

Lahoz, C., Schaefer, E. J., Cupples, L. A., Wilson, P. W. F., Levy, D., Osgood, D., Parpos, S., Pedro-Botet, J., Daly, J. A., & Ordovas, J. M. (2001). Apolipoprotein E genotype and cardiovascular disease in the Framingham Heart Study. *Atherosclerosis*, *154*(3), 529–537. https://doi.org/10.1016/S0021-9150(00)00570-0

Lana, D., Ugolini, F., Nosi, D., Wenk, G. L., & Giovannini, M. G. (2017). Alterations in the interplay between neurons, astrocytes and microglia in the rat dentate gyrus in experimental models of neurodegeneration. *Frontiers in Aging Neuroscience*, *9*(SEP), 1–17. https://doi.org/10.3389/fnagi.2017.00296

Li, C., Zhao, R., Gao, K., Wei, Z., Yaoyao Yin, M., Ting Lau, L., Chui, D., & Cheung Hoi Yu, A. (2011). Astrocytes: Implications for Neuroinflammatory Pathogenesis of Alzheimers Disease. *Current Alzheimer Research*, *8*(1), 67–80. https://doi.org/10.2174/156720511794604543

Li, X., Liu, Y., Zhang, H., Ren, L., Li, Q., & Li, N. (2011). Animal models for the atherosclerosis research: A review. *Protein and Cell*, *2*(3), 189–201. https://doi.org/10.1007/s13238-011-1016-3

Li, Y., G Zhang, C., Wang, X. H., & Liu, D. H. (2016). Progression of atherosclerosis in ApoE-knockout mice fed on a high-fat diet. *European Review for Medical and Pharmacological Sciences*, *20*(18), 3863–3867.

Libby, P. (2000). Coronary artery injury and the biology of atherosclerosis: Inflammation, thrombosis, and stabilization. *American Journal of Cardiology*, *86*(8 SUPPL. 2), 3–8. https://doi.org/10.1016/S0002-9149(00)01339-4

Libby, P. (2012). History of Discovery : Inflammation in Atherosclerosis. *Arterioscler Thromb Vasc Biol.*, *32*(9), 2045–2051.

https://doi.org/10.1161/ATVBAHA.108.179705.History

Liu CC, Kanekiyo T, Xu H, B. G. (2013). Nat Rev Neurol. *Nature Reviews Neuroscience*, *9*(2), 106–118. https://doi.org/10.1038/nrneurol.2012.263.Apolipoprotein

Liu, L., Liu, J., Bao, J., Bai, Q., & Wang, G. (2020). Interaction of Microglia and Astrocytes in the Neurovascular Unit. *Frontiers in Immunology*, *11*. https://doi.org/10.3389/fimmu.2020.01024

Liu, W., Tang, Y., & Feng, J. (2011). Cross talk between activation of microglia and astrocytes in pathological conditions in the central nervous system. *Life Sciences*, *89*(5–6), 141–146. https://doi.org/10.1016/j.lfs.2011.05.011

Masmoudi-Kouki, O., Gandolfo, P., Castel, H., Leprince, J., Fournier, A., Dejda, A., Vaudry, H., & Tonon, M. C. (2007). Role of PACAP and VIP in astroglial functions. *Peptides*, *28*(9), 1753–1760. https://doi.org/10.1016/j.peptides.2007.05.015

Mathieu, P., Pibarot, P., & Després, J. P. (2006). Metabolic syndrome: The danger signal in atherosclerosis. *Vascular Health and Risk Management*, *2*(3), 285–302. https://doi.org/10.2147/vhrm.2006.2.3.285

Matias, I., Morgado, J., & Gomes, F. C. A. (2019). Astrocyte Heterogeneity: Impact to Brain Aging and Disease. *Frontiers in Aging Neuroscience*, *11*. https://doi.org/10.3389/fnagi.2019.00059

Matsumoto, M., Nakamachi, T., Watanabe, J., Sugiyama, K., Ohtaki, H., Murai, N., Sasaki, S., Xu, Z., Hashimoto, H., Seki, T., Miyazaki, A., & Shioda, S. (2016). Pituitary Adenylate Cyclase-Activating Polypeptide (PACAP) Is Involved in Adult Mouse Hippocampal Neurogenesis After Stroke. *Journal of Molecular Neuroscience*, *59*(2), 270–279. https://doi.org/10.1007/s12031-016-0731-x

Meir, K. S., & Leitersdorf, E. (2004). Atherosclerosis in the apolipoprotein E–deficient mouse. *Arteriosclerosis, Thrombosis, and Vascular Biology*, *24*(6), 1006–1014.

Miyata, A., Arimura, A., Dahl, R. R., Minamino, N., Uehara, A., Jiang, L., Culler, M. D., & Coy, D. H. (1989). Isolation of a novel 38 residue-hypothalamic

polypeptide which stimulates adenylate cyclase in pituitary cells. *Biochemical and Biophysical Research Communications*, *164*(1), 567–574. https://doi.org/10.1016/0006-291X(89)91757-9

Morales, I., GuzmÃ¡n-MartÃ-nez, L., Cerda-Troncoso, C., FarÃ-as, G. A., & Maccioni, R. B. (2014). Neuroinflammation in the pathogenesis of Alzheimerâ€™s disease. A rational framework for the search of novel therapeutic approaches. *Frontiers in Cellular Neuroscience*, *8*. https://doi.org/10.3389/fncel.2014.00112

Mulder, M., Blokland, A., Van Den Berg, D. J., Schulten, H., Bakker, A. H. F., Terwel, D., Honig, W., De Kloet, E. R., Havekes, L. M., Steinbusch, H. W. M., & De Lange, E. C. M. (2001). Apolipoprotein E protects against neuropathology induced by a high-fat diet and maintains the integrity of the blood-brain barrier during aging. *Laboratory Investigation*, *81*(7), 953–960. https://doi.org/10.1038/labinvest.3780307

Nakamachi, T., Farkas, J., Watanabe, J., Ohtaki, H., Dohi, K., Arata, S., & Shioda, S. (2011). Role of PACAP in Neural Stem/Progenitor Cell and Astrocyte: from Neural Development to Neural Repair. *Current Pharmaceutical Design*, *17*(10), 973–984. https://doi.org/10.2174/138161211795589346

Nakashima, Y., Plump, A. S., Raines, E. W., Breslow, J. L., & Ross, R. (1994). *the Arterial Tree*. 1113.

Nandha, K. A., Benito-Orfila, M. A., Smith, D. M., Ghatei, M. A., & Bloom, S. R. (1991). Action of pituitary adenylate cyclase-activating polypeptide and vasoactive intestinal polypeptide on the rat vascular system: effects on blood pressure and receptor binding. *Journal of Endocrinology*, *129*(1), 69–73. https://doi.org/10.1677/joe.0.1290069

Napoli, C., & Palinski, W. (2005). Neurodegenerative diseases: Insights into pathogenic mechanisms from atherosclerosis. *Neurobiology of Aging*, *26*(3), 293–302. https://doi.org/10.1016/j.neurobiolaging.2004.02.031

Neustadt, J. (2006). Western diet and inflammation. *Integrative Medicine*, *5*(4), 14–18.

Pekny, M., & Nilsson, M. (2005). Astrocyte activation and reactive gliosis. *Glia*,

50(4), 427–434. https://doi.org/10.1002/glia.20207

Pelletier, J., Suchet, L., Witjas, T., Habib, M., Guttmann, C. R. G., Salamon, G., Lyon-Caen, O., & Chérif, A. A. (2001). A longitudinal study of callosal atrophy and interhemispheric dysfunction in relapsing-remitting multiple sclerosis. *Archives of Neurology*, *58*(1), 105–111. https://doi.org/10.1001/archneur.58.1.105

Piedrahita, J. A., Zhang, S. H., Hagaman, J. R., Oliver, P. M., & Maeda, N. (1992). Generation of mice carrying a mutant apolipoprotein E gene inactivated by gene targeting in embryonic stem cells. *Proceedings of the National Academy of Sciences of the United States of America*, *89*(10), 4471–4475. https://doi.org/10.1073/pnas.89.10.4471

Prasad, K., & Kalra, J. (1993). Oxygen free radicals and hypercholesterolemic atherosclerosis: Effect of vitamin E. *American Heart Journal*, *125*(4), 958–973. https://doi.org/10.1016/0002-8703(93)90102-F

Rasbach, E., Splitthoff, P., Bonaterra, G. A., Schwarz, A., Mey, L., Schwarzbach, H., Eiden, L. E., Weihe, E., & Kinscherf, R. (2019). PACAP deficiency aggravates atherosclerosis in ApoE deficient mice. *Immunobiology*, *224*(1), 124–132. https://doi.org/10.1016/j.imbio.2018.09.008

Rasmussen, K. L. (2016). Plasma levels of apolipoprotein E, APOE genotype and risk of dementia and ischemic heart disease: A review. *Atherosclerosis*, *255*(4), 145–155. https://doi.org/10.1016/j.atherosclerosis.2016.10.037

Rat, D., Schmitt, U., Tippmann, F., Dewachter, I., Theunis, C., Wieczerzak, E., Postina, R., Leuven, F., Fahrenholz, F., & Kojro, E. (2011). Neuropeptide pituitary adenylate cyclase-activating polypeptide (PACAP) slows down Alzheimer's disease-like pathology in amyloid precursor protein-transgenic mice. *The FASEB Journal*, *25*(9), 3208–3218. https://doi.org/10.1096/fj.10-180133

Reglodi, D., Kiss, P., Lubics, A., & Tamas, A. (2011). Review on the Protective Effects of PACAP in Models of Neurodegenerative Diseases In Vitro and In Vivo. *Current Pharmaceutical Design*, *17*(10), 962–972. https://doi.org/10.2174/138161211795589355

Reglodi, Dóra, Tamás, A., Lubics, A., Szalontay, L., & Lengvári, I. (2004). Morphological and functional effects of PACAP in 6-hydroxydopamine-induced lesion of the substantia nigra in rats. *Regulatory Peptides*, *123*(1-3 SPEC. ISS.), 85–94. https://doi.org/10.1016/j.regpep.2004.05.016

Ringer, C., Büning, L.-S., Schäfer, M. K. H., Eiden, L. E., Weihe, E., & Schütz, B. (2013). PACAP signaling exerts opposing effects on neuroprotection and neuroinflammation during disease progression in the SOD1(G93A) mouse model of amyotrophic lateral sclerosis. *Neurobiology of Disease*, *54*, 32–42. https://doi.org/10.1016/j.nbd.2013.02.010

Rodríguez, J. J., Yeh, C.-Y., Terzieva, S., Olabarria, M., Kulijewicz-Nawrot, M., & Verkhratsky, A. (2014). Complex and region-specific changes in astroglial markers in the aging brain. *Neurobiology of Aging*, *35*(1), 15–23. https://doi.org/10.1016/j.neurobiolaging.2013.07.002

Rose, G., Lynch, G., & Cotman, C. W. (1976). Hypertrophy and redistribution of astrocytes in the deafferented dentate gyrus. *Brain Research Bulletin*, *1*(1), 87–92. https://doi.org/10.1016/0361-9230(76)90052-6

Rosenfeld, M. E., Polinsky, P., Virmani, R., Kauser, K., Rubanyi, G., & Schwartz, S. M. (2000). Advanced Atherosclerotic Lesions in the Innominate Artery of the ApoE Knockout Mouse. *Arteriosclerosis, Thrombosis, and Vascular Biology*, *20*(12), 2587–2592. https://doi.org/10.1161/01.ATV.20.12.2587

Seaborn, T., Masmoudi-Kouli, O., Fournier, A., Vaudry, H., & Vaudry, D. (2011). Protective Effects of Pituitary Adenylate Cyclase-Activating Polypeptide (PACAP) Against Apoptosis. *Current Pharmaceutical Design*, *17*(3), 204–214. https://doi.org/10.2174/138161211795049679

Shen, S., Gehlert, D. R., & Collier, D. A. (2013). PACAP and PAC1 receptor in brain development and behavior. *Neuropeptides*, *47*(6), 421–430. https://doi.org/10.1016/j.npep.2013.10.005

Sherwood, N. M., Krueckl, S. L., & Mcrory, J. E. (2000). The origin and function of the pituitary adenylate cyclase-activating polypeptide (PACAP)/glucagon superfamily. *Endocrine Reviews*, *21*(6), 619–670. https://doi.org/10.1210/er.21.6.619

Shoelson, S. E., Herrero, L., & Naaz, A. (2007). Obesity, Inflammation, and Insulin Resistance. *Gastroenterology*, *132*(6), 2169–2180. https://doi.org/10.1053/j.gastro.2007.03.059

Skoglösa, Y., Lewén, A., Takei, N., Hillered, L., & Lindholm, D. (1999). Regulation of pituitary adenylate cyclase activating polypeptide and its receptor type 1 after traumatic brain injury: Comparison with brain-derived neurotrophic factor and the induction of neuronal cell death. In *Neuroscience* (Vol. 90, Issue 1, pp. 235–247). https://doi.org/10.1016/S0306-4522(98)00414-X

Sofroniew, M. V., & Vinters, H. V. (2010). Astrocytes: Biology and pathology. *Acta Neuropathologica*, *119*(1), 7–35. https://doi.org/10.1007/s00401-009-0619-8

Sofroniew, M. V. (2015). Astrogliosis perspectives. *Cold Spring Harbor Perspectives in Biology*, *7*(2), 1–16. http://www.ncbi.nlm.nih.gov/pubmed/25380660%0Ahttp://www.pubmedcentral.nih.gov/articlerender.fcgi?artid=PMC4315924

Sonoda, K., Matsui, T., Bito, H., & Ohki, K. (2018). Astrocytes in the mouse visual cortex reliably respond to visual stimulation. *Biochemical and Biophysical Research Communications*, *505*(4), 1216–1222. https://doi.org/10.1016/j.bbrc.2018.10.027

Splitthoff, P., Rasbach, E., Neudert, P., Bonaterra, G. A., Schwarz, A., Mey, L., Schwarzbach, H., Eiden, L. E., Weihe, E., & Kinscherf, R. (2020). PAC1 deficiency attenuates progression of atherosclerosis in ApoE deficient mice under cholesterol-enriched diet. *Immunobiology*, *225*(3), 151930. https://doi.org/10.1016/j.imbio.2020.151930

Stumm, R., Kolodziej, A., Prinz, V., Endres, M., Wu, D. F., & Höllt, V. (2007). Pituitary adenylate cyclase-activating polypeptide is up-regulated in cortical pyramidal cells after focal ischemia and protects neurons from mild hypoxic/ischemic damage. *Journal of Neurochemistry*, *103*(4), 1666–1681. https://doi.org/10.1111/j.1471-4159.2007.04895.x

Suleymanova, I., Balassa, T., Tripathi, S., Molnar, C., Saarma, M., Sidorova, Y., & Horvath, P. (2018). A deep convolutional neural network approach for astrocyte detection. *Scientific Reports*, *8*(1), 1–7.

https://doi.org/10.1038/s41598-018-31284-x

Tan, Y.-V., Abad, C., Lopez, R., Dong, H., Liu, S., Lee, A., Gomariz, R. P., Leceta, J., & Waschek, J. A. (2009). Pituitary adenylyl cyclase-activating polypeptide is an intrinsic regulator of Treg abundance and protects against experimental autoimmune encephalomyelitis. *Proceedings of the National Academy of Sciences*, *106*(6), 2012–2017. https://doi.org/10.1073/pnas.0812257106

Tedgui, A., & Mallat, Z. (2006). Cytokines in atherosclerosis: Pathogenic and regulatory pathways. *Physiological Reviews*, *86*(2), 515–581. https://doi.org/10.1152/physrev.00024.2005

Tracy, R. P. (1997). Atherosclerosis, thrombosis and inflammation: A problem of linkage. *Fibrinolysis and Proteolysis*, *11*(SUPPL. 1), 137–141. https://doi.org/10.1016/S0268-9499(97)80040-9

Usui, F., Shirasuna, K., Kimura, H., Tatsumi, K., Kawashima, A., Karasawa, T., Hida, S., Sagara, J., Taniguchi, S., & Takahashi, M. (2012). Critical role of caspase-1 in vascular inflammation and development of atherosclerosis in Western diet-fed apolipoprotein E-deficient mice. *Biochemical and Biophysical Research Communications*, *425*(2), 162–168. https://doi.org/10.1016/j.bbrc.2012.07.058

Utermann, G., Hees, M., & Steinmetz, A. (1977). Polymorphism of apolipoprotein E and occurrence of dysbetalipoproteinaemia in man. *Nature*, *269*(5629), 604–607. https://doi.org/10.1038/269604a0

Utermann, G., Kindermann, I., Kaffarnik, H., & Steinmetz, A. (1984). Apolipoprotein E phenotypes and hyperlipidemia. *Human Genetics*, *65*(3), 232–236. https://doi.org/10.1007/BF00286508

Vaudry, D., Falluel-Morel, A., Bourgault, S., Basille, M., Burel, D., Wurtz, O., Fournier, A., Chow, B. K. C., Hashimoto, H., Galas, L., & Vaudry, H. (2009). Pituitary adenylate cyclase-activating polypeptide and its receptors: 20 Years after the discovery. *Pharmacological Reviews*, *61*(3), 283–357. https://doi.org/10.1124/pr.109.001370

Walker, L. C., Parker, C. A., Lipinski, W. J., Callahan, M. J., Carroll, R. T., Gandy, S. E., Smith, J. D., Jucker, M., & Bisgaier, C. L. (1997). Cerebral lipid

deposition in aged apolipoprotein-E-deficient mice. *American Journal of Pathology*, *151*(5), 1371–1377.

Wang, G., Pan, J., Tan, Y. Y., Sun, X. K., Zhang, Y. F., Zhou, H. Y., Ren, R. J., Wang, X. J., & Chen, S. Di. (2008). Neuroprotective effects of PACAP27 in mice model of Parkinson's disease involved in the modulation of KATP subunits and D2 receptors in the striatum. *Neuropeptides*, *42*(3), 267–276. https://doi.org/10.1016/j.npep.2008.03.002

Waqar, A. B., Koike, T., Yu, Y., Inoue, T., Aoki, T., Liu, E., & Fan, J. (2010). High-fat diet without excess calories induces metabolic disorders and enhances atherosclerosis in rabbits. *Atherosclerosis*, *213*(1), 148–155. https://doi.org/10.1016/j.atherosclerosis.2010.07.051

Waschek, J. A. (2013). VIP and PACAP: Neuropeptide modulators of CNS inflammation, injury, and repair. *British Journal of Pharmacology*, *169*(3), 512–523. https://doi.org/10.1111/bph.12181

Więckowska-Gacek, A., Mietelska-Porowska, A., Wydrych, M., & Wojda, U. (2021). Western diet as a trigger of Alzheimer's disease: From metabolic syndrome and systemic inflammation to neuroinflammation and neurodegeneration. *Ageing Research Reviews*, *70*, 101397. https://doi.org/10.1016/j.arr.2021.101397

Williams, H., Johnson, J. L., Carson, K. G. S., & Jackson, C. L. (2002). Characteristics of intact and ruptured atherosclerotic plaques in brachiocephalic arteries of apolipoprotein E knockout mice. *Arteriosclerosis, Thrombosis, and Vascular Biology*, *22*(5), 788–792. https://doi.org/10.1161/01.ATV.0000014587.66321.B4

Yamada, H., Watanabe, M., & Yada, T. (2004). Cytosolic Ca2+ responses to sub-picomolar and nanomolar PACAP in pancreatic β-cells are mediated by VPAC2 and PAC1 receptors. *Regulatory Peptides*, *123*(1–3), 147–153. https://doi.org/10.1016/j.regpep.2004.03.020

Yarchoan, M., Xie, S. X., Kling, M. A., Toledo, J. B., Wolk, D. A., Lee, E. B., Van Deerlin, V., Lee, V. M. Y., Trojanowski, J. Q., & Arnold, S. E. (2012). Cerebrovascular atherosclerosis correlates with Alzheimer pathology in

neurodegenerative dementias. *Brain*, *135*(12), 3749–3756. https://doi.org/10.1093/brain/aws271

Yin, Y., & Wang, Z. (2018). *ApoE and Neurodegenerative Diseases in Aging* (pp. 77–92). https://doi.org/10.1007/978-981-13-1117-8_5

Zagami, A. S., Edvinsson, L., & Goadsby, P. J. (2014). Pituitary adenylate cyclase activating polypeptide and migraine. *Annals of Clinical and Translational Neurology*, *1*(12), 1036–1040. https://doi.org/10.1002/acn3.113

Zhang, S. H., Reddick, R. L., Piedrahita, J. A., & Maeda, N. (1992). Spontaneous hypercholesterolemia and arterial lesions in mice lacking apolipoprotein E. *Science*, *258*(5081), 468–471. https://doi.org/10.1126/science.1411543

8. Appendix

8.1. Descriptive analyses

Table 8. Means and standard deviations of astrocyte numbers.

Brain region	Genotype	Diet	*N*	*M*	*SD*
Corpus callosum	*WT*	SD	3	200.17	85.82
		HCD	4	43.88	187.73
	ApoE$^{-/-}$	SD	3	522.67	204.61
		HCD	4	713.75	215.17
	PACAP$^{-/-}$/*ApoE*$^{-/-}$	SD	4	512.38	198.24
		HCD	4	481.88	118.38
	PAC1$^{-/-}$/*ApoE*$^{-/-}$	SD	4	597.55	225.93
		HCD	4	595.75	186.63
Dentate gyrus	*WT*	SD	3	462.5	240.64
		HCD	4	693.00	213.01
	ApoE$^{-/-}$	SD	3	627.17	133.09
		HCD	4	1051.38	337.28
	PACAP$^{-/-}$/*ApoE*$^{-/-}$	SD	4	679.38	256.29
		HCD	4	595.13	234.17
	PAC1$^{-/-}$/*ApoE*$^{-/-}$	SD	4	878.88	352.55
		HCD	4	812	186.75
Visual cortex	*WT*	SD	3	10.33	13.14
		HCD	4	23.63	29.96
	ApoE$^{-/-}$	SD	3	25.33	17.62
		HCD	4	40.13	34.65
	PACAP$^{-/-}$/*ApoE*$^{-/-}$	SD	4	19.38	8.63
		HCD	4	23.13	13.44
	PAC1$^{-/-}$/*ApoE*$^{-/-}$	SD	4	12.63	9.2

	HCD	4	22.13	21.75

Note. *N* = Number of brain slices.

Table 9. Means and standard deviations of the proportional area of astrocytes.

Brain region	Genotype	Diet	*N*	*M*	*SD*
Corpus callosum	*WT*	SD	3	5.1	2.3
		HCD	4	11.15	4.26
	ApoE$^{-/-}$	SD	3	10.3	2.65
		HCD	4	15.33	5.14
	PACAP$^{-/-}$/*ApoE*$^{-/-}$	SD	4	10.75	6.22
		HCD	4	11.1	2.16
	PAC1$^{-/-}$/*ApoE*$^{-/-}$	SD	4	11.0	7.45
		HCD	4	12.38	4.32
Dentate gyrus	*WT*	SD	3	5.98	1.01
		HCD	4	9.18	1.11
	ApoE$^{-/-}$	SD	3	9.43	.59
		HCD	4	13.58	3.2
	PACAP$^{-/-}$/*ApoE*$^{-/-}$	SD	4	9.83	5.12
		HCD	4	12.25	.55
	PAC1$^{-/-}$/*ApoE*$^{-/-}$	SD	4	10.55	3.74
		HCD	4	12.7	3.85
Visual cortex	*WT*	SD	3	2.2	2.51
		HCD	4	2.6	1.91
	ApoE$^{-/-}$	SD	3	2.3	1.41
		HCD	4	4.78	3.45
	PACAP$^{-/-}$/*ApoE*$^{-/-}$	SD	4	2.18	1.16
		HCD	4	2.43	.48
	PAC1$^{-/-}$/*ApoE*$^{-/-}$	SD	4	2.15	1.09
		HCD	4	1.95	1.66

Note. *N* = Number of brain slices; *M* and *SD* in %

8.2. Verzeichnis der akademischen Lehrer/-innen

Meine akademischen Lehrenden waren in Marburg:

Althaus, Arweiler, Auschill, Bette, Braun, Cetin, Feuser, Fischer, Frankenberger, Gente, Glörfeld, Hellak, Himpel, Hoch, Höffken, Jablonski-Momeni, Korbmacher-Steiner, Kroh, Lill, Lotzmann, Mengel, Milani, Mittag, Moll, Mutters, Neff, Neumüller, Nonnenmacher, Pieper, Ramaswamy, Richter, Roggendorf, Steininger, Weber, Weihe, Westermann, Worzfeld, Wrocklage

8.3. Danksagung

Mein Dank gilt meinem Doktorvater Prof. Dr. E. Weihe, vor allem für die Überlassung des Dissertationsthemas, die konstruktive Hilfe und die freundliche Betreuung. Ebenso möchte ich mich bei allen Mitarbeitern der AG am Institut für Anatomie und Zellbiologie der Philipps-Universität Marburg, insbesondere bei Herrn Dr. Schäfer, Frau Zibuschka und Frau Unverzagt für Ihre Unterstützung im Labor und Beantwortung jeglicher Fragen, bedanken. Vor allem Annabel Vetterlein danke ich für die ständige Motivation und Unterstützung. Schließlich sei der Dank auch an meine Eltern und meinen Ehemann gerichtet, die während der gesamten Zeit hinter mir standen und mich stets in allen Belangen unterstützt haben.